Master's degree Course in Energy and Nuclear Engineering

Renewable Energy Engineering

POLITECNICO
DI TORINO

Master's Degree Thesis

Study of smoke behaviour caused by fires in tunnels due to electric vehicles in confined spaces

Andrea Fantini

Supervisor
Prof. Papurello Davide

Politecnico di Torino
July 2023

Abstract

Electric machines and batteries play a vital role in contemporary technology, providing power for various devices from smartphones to electric cars. Nevertheless, they also pose a potential fire hazard, especially in the case of lithium-ion batteries, which are widely utilized in numerous electronic gadgets. Currently, the study of fire evolution using Fire Safety Engineering methods is becoming increasingly significant in Italy and other developed nations.

To tackle this problem, researchers and engineers have been dedicated to enhancing fire prevention and suppression systems. One such system is the software Pyrosim, which employs computational modelling to simulate and analyse fires in enclosed environments like buildings or tunnels. By combining Pyrosim with FDS as a simulation method, a more comprehensive understanding of fire behaviour can be achieved.

This thesis, built upon the previous research conducted in the field of fire safety for electric vehicles and batteries, simulates the behaviour within a tunnel in the case of fire caused by an electric vehicle.

Through simulations with varying parameters such as ventilation and emergency exit, it was possible to analyse how fires behave in enclosed spaces and identify potential weaknesses in fire suppression systems. Furthermore, the investigation of temperature and heat released during simulated fires aids in gaining a better understanding of the specific risks associated with electric vehicles.

In conclusion, the findings underscore the significance of ongoing research and development in fire prevention and suppression systems. By utilizing advanced modelling tools like Pyrosim, it becomes feasible to improve our understanding of fire behaviour in enclosed spaces and work towards enhancing the safety of these technologies.

Table of Contents

List of Tables

List of Figures

Nomenclature

HOC: Heat of combustion

BEV: battery electric vehicle

HRR: Heat release rate

LFL: Lower flammability limit

OSU: Ohio State University

PHRR: Peak heat release rate

SOC: State of charge

THR: Total heat release

EU: European Union

FDS: Fire Dynamic Simulator

GISS: Goddard Institute for Space Studie

THCP: Thermocouple

1. Introduction

Electrification of transportation has become a crucial step in mitigating climate change, as the sector of transportation accounts for a significant portion of greenhouse gas emissions. However, safety is associated with the use of Li-ion batteries because of posing a challenge in their widespread adoption. Several incidents in the past have highlighted the risks associated with Li-ion batteries, such as the Samsung Galaxy Note 7 fiasco, which resulted in product recalls and bans on air travel. Research is focused on developing more stable battery materials, such as solid-state batteries, which have the potential to eliminate the risks associated with liquid electrolytes. Another approach is to develop advanced battery management systems that can detect and prevent potential hazards. In addition to these technological solutions, regulations and guidelines are being developed to ensure the safe use and transportation of Li-ion batteries. Another important aspect that needs to be addressed is the issue of battery disposal, which can pose environmental and health hazards. Recycling and reuse of batteries can minimize these risks and promote a circular economy. In conclusion, while Li-ion batteries offer significant advantages in terms of energy and power capacities, safety concerns need to be addressed to ensure their sustainable and widespread use in transportation and other applications. [1]

2. Global warming

The temperature of the Earth's atmosphere has been increasing since the advent of the Industrial Revolution. Although natural variability contributes to this trend, the overwhelming evidence suggests that human activities, particularly the release of greenhouse gases that trap heat, are primarily responsible for the warming of our planet.

NASA's Goddard Institute for Space Studies (GISS) has been conducting an ongoing analysis of global temperature, which reveals that the Earth's average temperature has risen by at least 1.1°C since 1880. Most of the warming has occurred since 1975, with a rate of increase of approximately 0.15 to 0.20°C per decade.

The image below displays the global temperature anomalies in 2022, which tied with previous years as the fifth-warmest year on record. The last nine years have been the warmest since modern recordkeeping began in 1880.

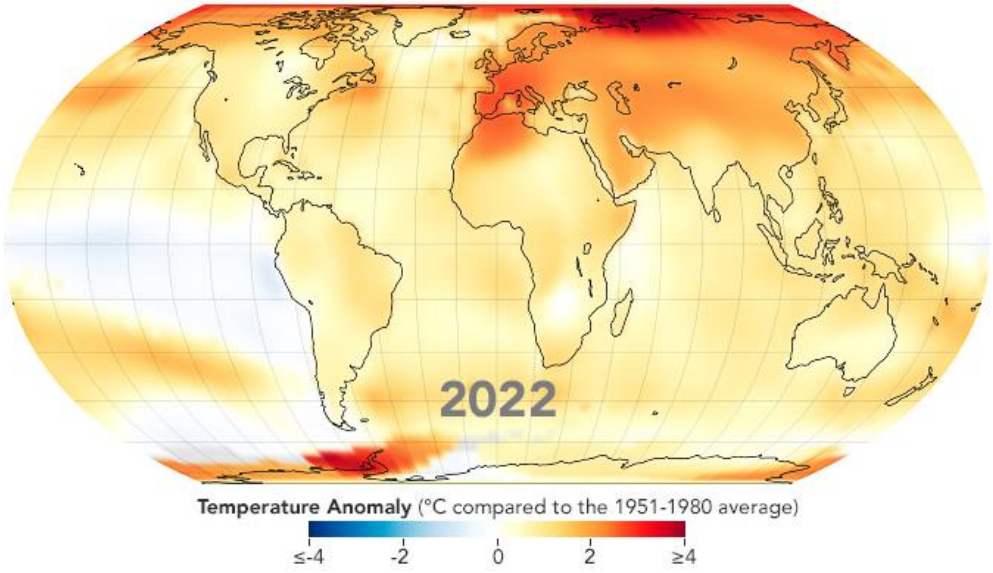

Figure 1

As the maps show, global warming does not mean temperatures rise everywhere at every time by same rate. Temperatures might rise 5 degrees in one region and drop 2 degrees in another. For instance, exceptionally cold winters in one place might be balanced by extremely warm winters in another part of the world. Generally, warming is greater over land than over the oceans because water is slower to absorb and release heat (thermal inertia). Warming may also differ substantially within specific land masses and ocean basins. In the animation at the

top of the page and in the bar chart below, the years from 1880 to 1939 tend to be cooler, then level off by the 1950s. Decades within the base period (1951-1980) do not appear particularly warm or cold because they are the standard against which other years are measured. The levelling off of temperatures in the middle of the 20th century can be explained by natural variability and by the cooling effects of aerosols generated by factories, power plants, and motor vehicles in the years of rapid economic growth after World War II. Fossil fuel use also increased after the war (5 percent per year), boosting greenhouse gases. Cooling from aerosol pollution happened rapidly. In contrast, greenhouse gases accumulated slowly, but they remain in the atmosphere for a much longer time. According to former GISS director James Hansen, the strong warming trend of the past four decades likely reflects a shift from balanced aerosol and greenhouse gas effects on the atmosphere to a predominance of greenhouse gas effects after aerosols were curbed by pollution controls.

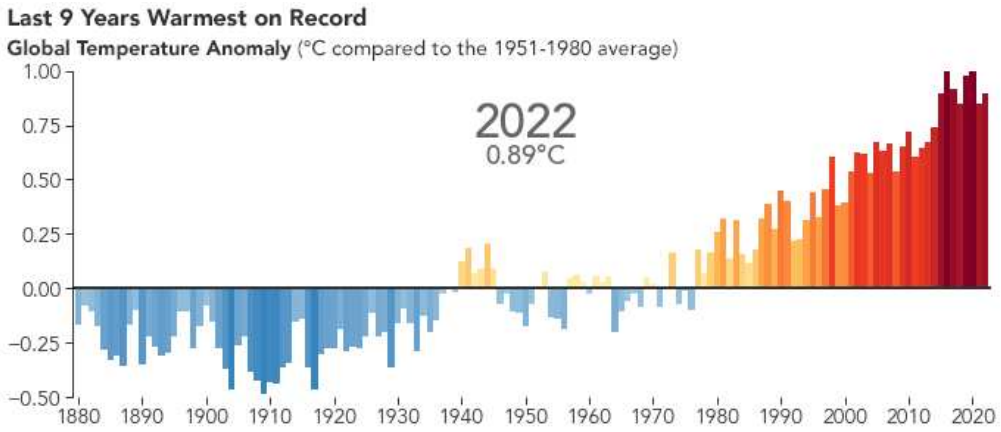

Figure 2

Why should we care about one or two degrees of global warming? After all, temperatures fluctuate by many degrees every day where we live.

The temperatures we experience locally and in short periods can fluctuate significantly due to predictable, cyclical events (night and day, summer and winter) and hard-to-predict wind and precipitation patterns. But the global temperature mainly depends on how much energy the planet receives from the Sun and how much it radiates back into space. The energy coming from the Sun fluctuates very little by year, while the amount of energy radiated by Earth is closely tied to the chemical composition of the atmosphere particularly the amount of heat-trapping greenhouse gases.

A one-degree global change is significant because it takes a vast amount of heat to warm all of the oceans, the atmosphere, and the land masses by that much. In the past, a one- to two-degree drop was all it took to plunge the Earth into the Little Ice Age. A five-degree drop was enough to bury a large part of North America under a towering mass of ice 20000 years ago.

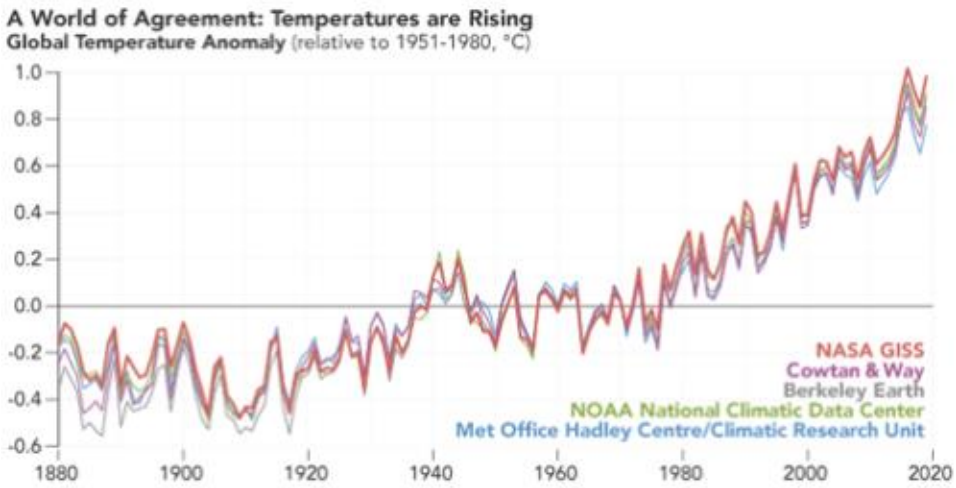

Figure 3

Global temperature data has been recorded since 1880, but it was limited due to inadequate observation coverage across the planet before that time. The chart displayed above illustrates yearly temperature anomalies from 1880 to 2020 as documented by various organizations including NASA, NOAA, Berkeley Earth research group, Met Office Hadley Centre (UK), and the Cowtan and Way analysis. Despite minor year-to-year variations, all five records display consistent peaks and valleys. They all indicate a rapid warming trend in recent decades, with the last decade being the warmest.

NASA GISS team established the 1951-1980 period as its baseline, mainly because the U.S. National Weather Service considers a three-decade period as the norm for average temperature. Additionally, GISS's temperature analysis effort began around 1980, making 1951-1980 the most recent 30-year period. The team's goal is to provide an estimate of temperature change that can be compared with global climate change predictions in response to atmospheric carbon dioxide, aerosols, and changes in solar activity.

NASA's temperature analyses incorporate surface temperature measurements from over 20000 weather stations, sea surface temperature observations from ships and buoys, and temperature data from Antarctic research stations. These in situ measurements are evaluated using an algorithm that accounts for the diverse spacing of temperature stations around the world and urban heat island effects.

[2] [3] [4] [5] [6] [7]

3. Electric vehicles

3.1 The transport electrification

Transportation is a major contributor to the greenhouse gas emissions responsible for climate change. In 2019, it accounted for 23% of energy-related carbon dioxide emissions worldwide and 29% of all greenhouse gas emissions in the United States.

The ongoing systemic shifts in the transportation industry have the potential to decrease the sector's greenhouse gas emissions. However, the question remains whether these changes will be sufficient to significantly reduce emissions.

The Intergovernmental Panel on Climate Change released a new report on April 4, 2022, in which scientists from across the globe assessed the most recent research on measures to address climate change. The report indicates that the cost reduction of renewable energy and electric vehicle batteries, along with policy modifications, has slowed the growth of climate change over the last decade. Nonetheless, immediate and substantial reductions are necessary to halt the expansion of emissions entirely and prevent unchecked global warming.

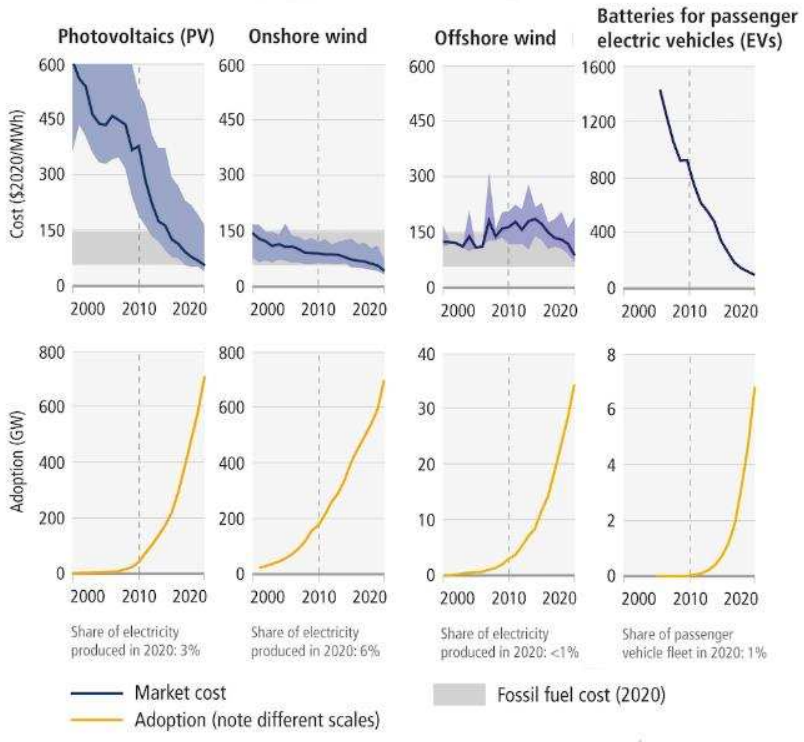

Figure 4

The adoption of all-electric vehicles has seen a remarkable increase since the launch of the Tesla Roadster and Nissan Leaf a little over a decade ago, following the success of hybrid vehicles.

In 2021, the global sales of electric passenger vehicles, comprising plug-in hybrids, doubled, reaching 6.6 million units, which accounted for about 9% of all car sales that year.

Stringent regulatory policies have promoted the production and adoption of electric vehicles, including California's Zero Emission Vehicle regulation, which mandates automakers to manufacture a specific number of zero-emission vehicles based on their total vehicles sold in California; the European Union's CO2 emissions criteria for new vehicles; and China's New Energy Vehicle policy, all of which have helped drive the widespread adoption of EVs we witness today.

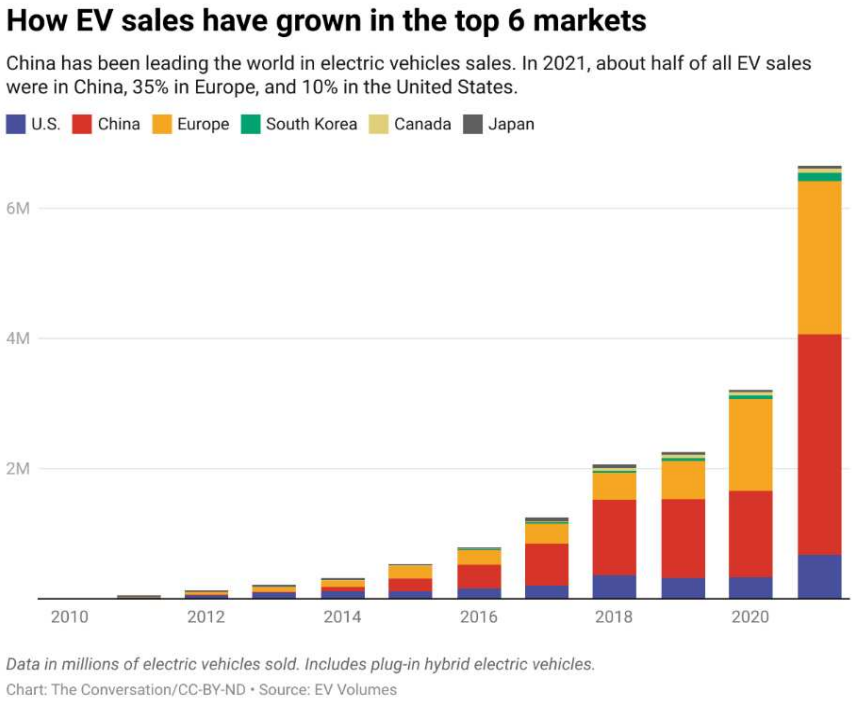

Figure 5

Apart from passenger cars, several micro-mobility choices, such as e-rickshaws, electric scooters, bikes, and buses, have also been electrified. As the cost of lithium-ion batteries continues to fall, these transportation alternatives will become more affordable and contribute to an increased uptake of battery-powered vehicles that previously relied on fossil fuels.

It's important to bear in mind that the effectiveness of the shift toward electric transportation in cutting greenhouse gas emissions ultimately depends on how clean the power grid is. For instance, China aims to have 20% of its vehicles running on electricity by 2025, but its electricity grid still relies heavily on coal.

As the world shifts toward more renewable energy, these vehicles will eventually produce fewer carbon emissions. There are also numerous developing and potentially promising added benefits of electromobility when integrated with the power system. The batteries in electric vehicles have the potential to act as storage devices for the grid, which can help stabilize the variability of renewable energy resources in the power sector, among many other advantages. [8]

Navigating the realm of electric vehicles can be challenging, but it's possible to categorize them into these fundamental groups:

- EV/BEV: Battery-powered electric cars, also known as EVs or BEVs, solely rely on an electric motor fueled by rechargeable batteries. They can be charged at home with a standard outlet or quickly at a charging station.
- HEV: Hybrid electric vehicles utilize both an electric motor and a gasoline-powered internal combustion engine. Although they can't be charged by plugging in, their batteries can be charged by regenerative braking and the gas engine as they're driven.
- PHEV: Plug-in hybrid electric vehicles are a type of hybrid electric car that can be charged by plugging in. They generally have a greater all-electric range than traditional hybrids.
- EREV: Extended-range electric vehicles are hybrids designed to operate entirely on electric motors and don't include an internal combustion engine. Instead, they have a gas generator that can produce electricity to power the batteries and motor when required to expand the range.
- FCEV: Fuel cell electric vehicles differ from other electric cars in that they use fuel cells to generate electricity through a reaction between hydrogen and oxygen. They need to be refueled at hydrogen charging stations. [9]

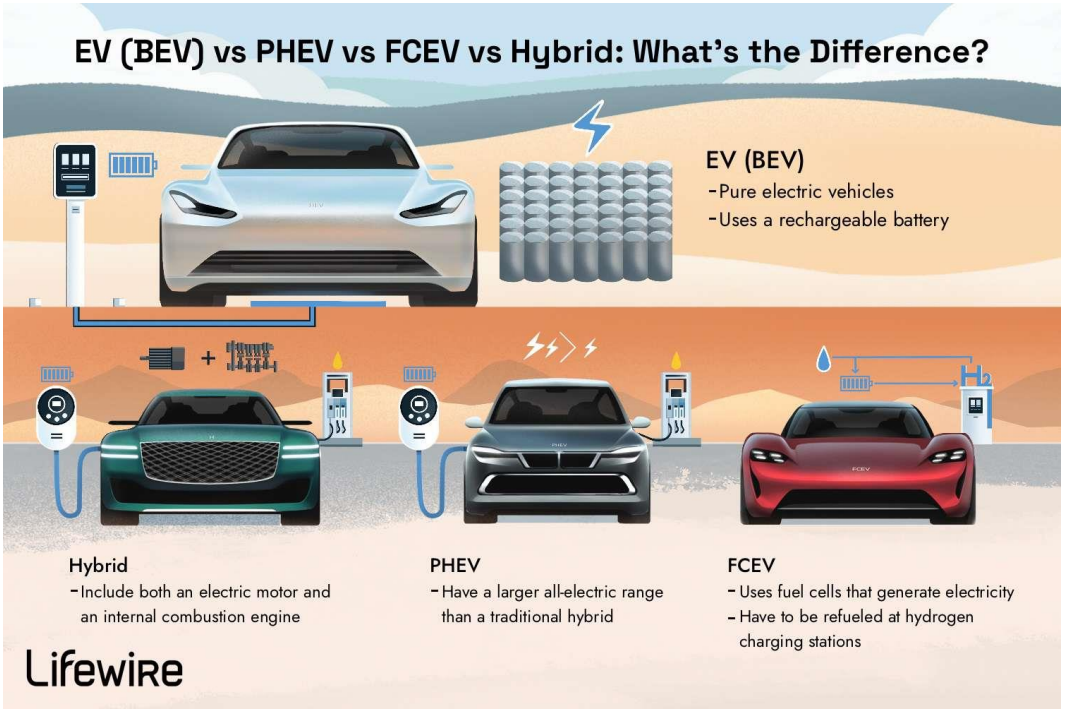

Figure 6

3.2 BEV

Battery-powered electric vehicles have emerged as a prominent player in the contemporary automotive industry. There are various types of batteries employed in the fabrication of modern-day EVs, making it challenging to determine the optimal choice that aligns with the most crucial characteristics from different standpoints, including energy storage efficiency, construction specifications, price, safety, and useful lifespan. In particular, electric vehicle can utilize four different battery types: Lithium-Ion (Li-Ion), Molten Salt (Na-NiCl2), Nickel Metal Hydride (Ni-MH), and Lithium Sulphur (Li-S), with an identical energy storage capacity. [10]

Li-Ion batteries are currently the most widely used technology in electric vehicles, mainly due to their high energy density and power per unit mass. This has enabled the development of lighter and smaller batteries at competitive prices.

Li-Ion batteries have higher power (800 … 2000 W/kg) and specific energy (100 … 250 Wh/kg) than Ni-MH batteries.

Li-Ion technology is the best "charge to weight" solution and meets the most important requirements for batteries used in the electric vehicle industry. In addition, Li-Ion batteries do not have a memory effect, which can gradually decrease the maximum energy capacity with repeated charging without being completely discharged, resulting in a longer lifespan.

However, the high operating temperature required by Li-Ion batteries can affect energy performance, lifespan, and safety during use. To control and monitor the internal cell temperature, this technology requires a battery management system. Other disadvantages of Li-Ion batteries include high production costs, low recycling capacity of used batteries, and inadequate recharging infrastructure.

At the beginning of 2000, Ni-MH batteries were considered the most advanced technology used in hybrid and electric vehicles, representing the first step toward today's technology. Ni-MH technology met the requirements for batteries developed for the automotive industry, including high energy density and power, resulting in a range of over 300 km with batteries with 70 Wh/kg specific energy. These batteries can be used in propulsion systems equipped with electric engines of 320 V AC or 180 V DC, and have a longer lifespan (up to 80% Depth of Discharge DOD). Other advantages include the ability to use regenerative energy recovered from braking, the use of recyclable materials in their development, excellent thermal properties (operating temperature starting from – 30 °C up until + 70 °C), and battery charging and discharging safety, among others. A comparison between Li-Ion and NiMH batteries conducted by showed that, from a cell point of view, Li-Ion cells offer a 20% increase in specific energy. However, considering the entire battery system with the added weight of the battery management system in Li-Ion technology, the Ni-MH battery has a simpler management system and reduced weight. The Nissan Leaf EV, equipped with a Li-Ion battery, has an autonomy of 160 km, while the GM electric car, EV1, equipped with a Ni-MH battery, has an autonomy of 280 km, making Ni-MH batteries more efficient from an autonomy point of view. The disadvantages of Ni-MH batteries include increased weight and obsolete technology.

Recent research in electric vehicle battery technology has resulted in the development of other battery types, including Na-NiCl2 batteries, also known as ZEBRA batteries (Zeolite Battery Research Africa). These batteries were used to equip some concept cars and buses used in urban public transportation. These

batteries are notable for their high energy density (90 … 120 WH/kg) and lower price compared to other existing technologies. Other advantages include overcharge and over-discharge resistance, increased cycle life, and structural robustness, allowing for their use in harsh environments without being affected by low temperatures.

However, Na-NiCl2 batteries have a major drawback in the form of high internal operating temperatures (270 °C … 350 °C), and continuous use of the electric vehicle is necessary to prevent the battery electrolyte from freezing. If the car is not used, an external heating system is required to maintain the system at the operating temperature, consuming 90 Wh power from the battery. [10]

3.3 Lithium-Ion batteries

Lithium-ion batteries are widely used in portable electronic devices such as smartphones, laptops, and tablets, as well as electric vehicles and grid energy storage systems. They offer high energy density, long cycle life, and low self-discharge, making them a popular choice for a variety of applications.

The charging and discharging process of lithium-ion batteries is based on the movement of lithium ions between the positive and negative electrodes. During discharge, the lithium ions move from the negative to the positive electrode through the electrolyte, producing an electrical current that can be used to power a device. During charging, the process is reversed, and the lithium ions move from the positive to the negative electrode, where they are stored until needed.

One important consideration in the design and use of lithium-ion batteries is safety, as they have been known to catch fire or explode if they are damaged or subjected to extreme temperatures. To mitigate these risks, manufacturers typically incorporate a number of safety features, including thermal management systems, voltage regulators, and protective circuits.

In recent years, there has been growing interest in the development of new types of lithium-ion batteries with improved performance and safety characteristics. This includes the use of new electrode materials, such as silicon, and the development of solid-state electrolytes, which could offer higher energy density and reduced risk of fire or explosion. [11]

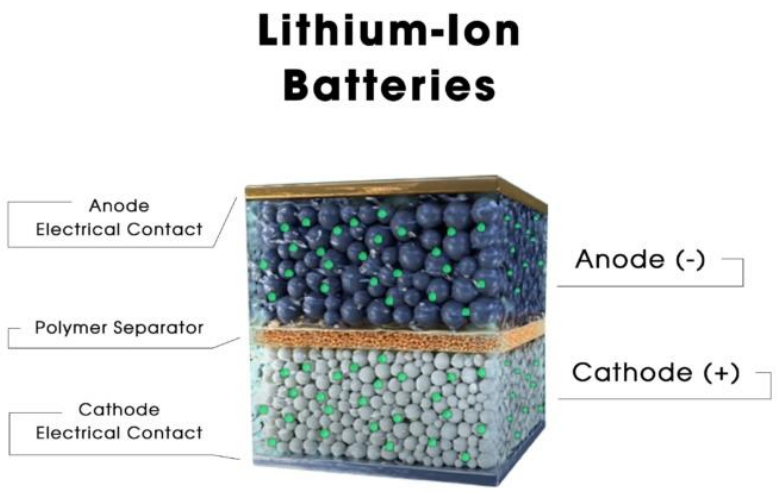

Figure 7

To charge a single Li-ion cell, a two-stage process is used, consisting of a constant current (CC) phase followed by a constant voltage (CV) phase. For a complete Li-ion battery, a three-stage process is employed, including a balance phase to ensure that the state of charge of each cell is balanced. During the CC phase, the charger provides a constant current to the battery while gradually increasing the voltage. During the balance phase, the charging current is decreased while a balancing circuit balances the state of charge of each individual cell. Finally, during the CV phase, the charger applies a voltage to the battery equal to the maximum cell voltage times the number of cells in series, as the current gradually decreases towards zero and eventually falls below a predetermined threshold of about 3% of the initial constant charge current.

In the case of an electric vehicle, while driving (discharge phase), lithium ions from the negative electrode flow through the separator to the positive electrode, providing the required amount of electrical energy to the electric motor. Electrons travel outside the battery via an electrical cable connection from the negative electrode's collector (copper) to the positive electrode's collector (aluminium). Charging an electric vehicle at a charging station reverses this process, with lithium ions moving back from the positive to the negative electrode and being reincorporated into the graphite.

To achieve the necessary power characteristics for entirely electric driving, numerous lithium-ion cells must be coupled together. As a result, the car battery is constructed by assembling a number of basic cells into a module and then several modules into a battery system.

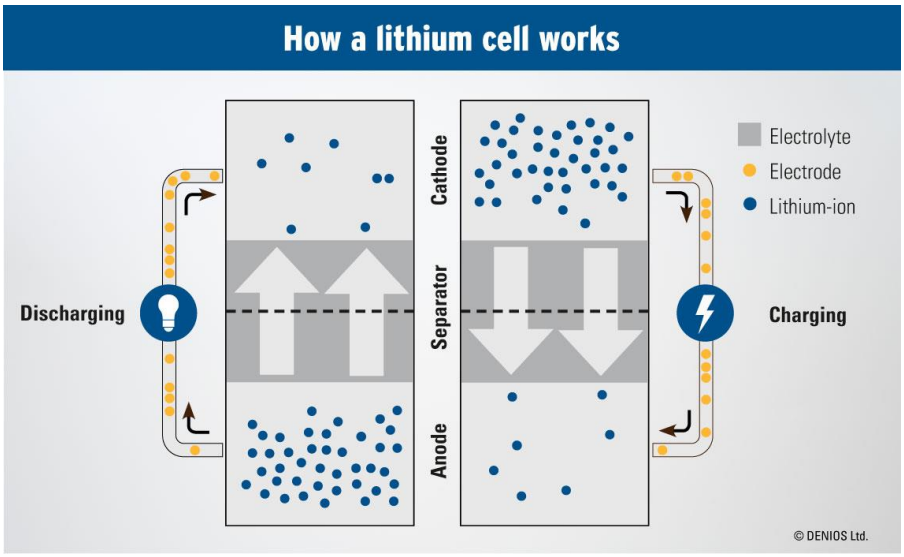

Figure 8

To summarize, the choice of materials for the electrodes, separator, and electrolyte greatly affects the performance and safety of lithium-ion batteries. While various materials are being studied, only a few are currently commercialized. Carbon/graphite is the most frequently used anode material, but alloy anodes made of aluminium, tin, magnesium, silver, antimony and their alloys are also used to address capacity and safety issues. For the cathode, cobalt was initially used but nickel is now more commonly used due to problems associated with cobalt. Typically the separator is a polymer made from materials such as polyethylene or polypropylene, and can be strengthened with ceramics to allow physical stability at higher temperatures. The electrolyte is a mixture of a Li-salt, organic solvents, and additives with specific characteristics such as high ionic conductivity, high cation-transfer capability, wide electrochemical stability window, high thermal stability and mechanical strength, and low-cost to manufacture.

3.4 Disadvantages

Despite their technological promise, Li-ion batteries still have a number of shortcomings, particularly when it comes to safety. Li-ion batteries have a tendency to overheat and can be damaged at high voltages, which can lead to thermal runaway and combustion. This has caused significant problems, such as the grounding of the Boeing 787 fleet following reports of onboard battery fires. Due to the risks associated with Li-ion batteries, several shipping companies refuse to perform bulk shipments of batteries by plane. Safety mechanisms are required to limit voltage and internal pressures, which can increase weight and limit performance in some cases. Additionally, Li-ion batteries are subject to aging, which means they can lose capacity and often fail after several years. Another factor that limits their widespread adoption is their cost, which is approximately 40% higher than Ni-Cd. Addressing these issues is a crucial component of current research into the technology. Finally, even though Li-ion batteries have high energy density compared to other types of batteries, they are still only about a hundred times less energy-dense than gasoline (which has a mass energy density of 12700 Wh/kg or a volume energy density of 8760 Wh/L). [12]

4. Fire risk

4.1 Combustion

Combustion is defined as a chemical process where a substance that can be oxidized, known as a fuel, reacts with an oxidizing substance, called a comburent. During this reaction, energy is released, often in the form of heat, as electrons transfer from the fuel to the comburent. The products of this reaction have less energy than the initial reactants, and this difference in energy is what generates the heat that is released.

The most common fuels that undergo combustion are substances that contain high levels of hydrogen and carbon. These fuels can be found in various states, including solid, liquid, and gas, and include materials such as wood, oil, and natural gas derivatives. The comburent, on the other hand, is usually oxygen, which is present in the air.

As the combustion reaction takes place, the temperature rises, and electromagnetic waves are emitted in the visible spectrum, resulting in the appearance of flames in the reaction zone. Consequently, after combustion occurs, heat, flames, gases, and smoke are produced.

The damage caused by fire cannot be predicted beforehand as the activation and propagation of fire depends on several random variables, such as the ignition phase, development, fuel quantity and distribution, geometric characteristics, and ventilation conditions. Therefore, the only reliable methods of studying fires are through assessing the probability of risk, numerical simulations, and experimental tests.

4.2 Compartment Fire

The phrase "compartment fire" is a commonly used term to refer to a fire that occurs in a confined space, such as a room or compartment within a building. If the fire is allowed to burn until all available fuel and ventilation are exhausted, it will pass through three main stages:

1. The initial stage, or preflashover, during which the fire remains localized in the area of its origin and the average temperature in the compartment remains relatively low.
2. The fully developed stage, or postflashover, during which all combustible materials are consumed, and flames can be seen filling the entire volume of the compartment, including ventilation openings.

3. The decay period, during which the fire begins to subside as the available fuel is consumed. This stage is identified when the average temperature falls to 80% of the maximum temperature achieved during the fully developed stage.

These stages are depicted in Figure 9, which shows the fire size (measured in terms of the rate of heat release in kW) as a function of time. During the initial stage, the average temperature in the lower portion of the compartment remains relatively low, although a layer of hot smoke accumulates under the ceiling and increases in depth and temperature as the fire grows. The development of this layer is a crucial factor in the progression of the fire to the fully developed stage. However, a fire can self-extinguish if the first ignited material burns out before other items are involved or be suppressed if it lacks air (oxygen) supply. This can happen in spaces with insufficient ventilation, such as closed and tightly fitting doors and windows. [13]

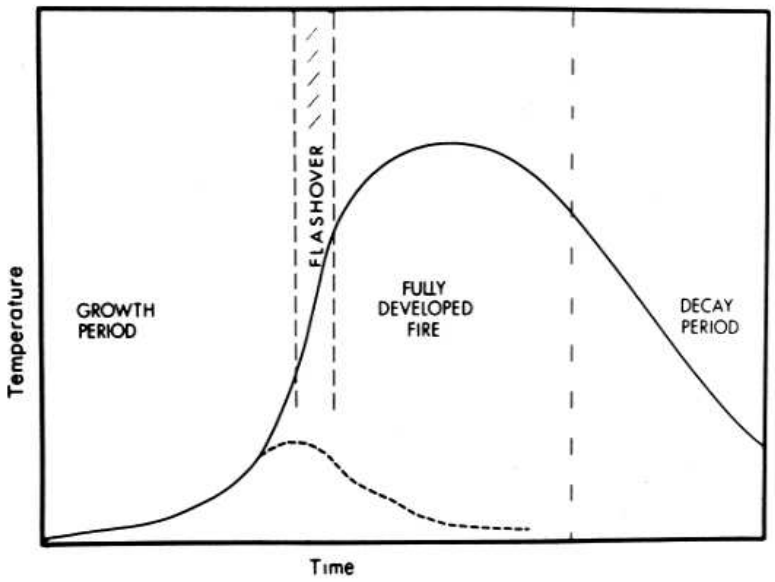

Figure 9

4.3 Fire Phases

This situation has the potential to be dangerous for firefighters and others present. When there is a lack of oxygen, the fuel may continue to burn slowly and inefficiently, creating flammable fumes that will collect in the compartment. If someone opens a door or a window breaks, fresh air rushes in and hot fire products flow out. The fire will intensify, and the trapped flammable fumes will burn rapidly as they mix with the air, creating a fireball that could seriously harm anyone in its path. This occurrence is commonly known as "backdraft."
If the compartment has good ventilation and enough flammable material, a fire that has started can quickly become fully developed.
When a fire transitions from the growth phase to the fully developed phase, it's called flashover. Those who haven't left the compartment before flashover are unlikely to survive, as high temperatures and intense radiant heat quickly develop, along with high levels of toxic and harmful gases. Individuals in other areas of the same building are also in danger immediately after flashover happens in the room of origin. If there's a path through which the heat, smoke, and toxic gases can enter corridors, escape routes, and stairwells, the rapidly burning fully developed fire can produce untenable levels of heat, smoke, and toxic gases. As a result, it's crucial to evacuate the building's occupants as soon as possible after a fire starts. Early detection raises the possibility of a successful evacuation, but this could be jeopardized if the fire's growth period is short. As a result, identifying situations that could cause rapid fire growth and designing spaces and selecting their contents to lengthen the time to flashover in the event of a fire is critical.

The sequence leading from ignition to flashover is characterized by a fire that gradually becomes more intense (rate of heat release). The layer of hot, smoky gases that accumulates beneath the ceiling causes the upper surfaces of the compartment to become hot. These surfaces and the smoke layer radiate downward, heating the combustible materials at low levels at a rate that increases as the fire grows in size. This results in an increase in burning rates and a high rate of flame spread over flammable surfaces. Flashover occurs when the fire quickly spreads to engulf all of the flammable materials in the compartment.
This phenomenon is illustrated in Fig. 10, which compares the burning rates of two poly (methyl methacrylate) slabs, one burning in an unconfined atmosphere and the other under a hood meant to simulate the confinement provided by the compartment's ceiling. The presence of the hood deflects the fire plume and eventually creates a reservoir of hot burning gas, which acts as a strong source of radiant heat ($\dot{Q}''_E$) for the horizontal fuel slab. Not only is the final burning rate several times greater than that of the free-burning slab, but the development rate is also greatly increased. This behaviour is believed to be typical of the processes that occur during the development of a real compartment fire. [13]

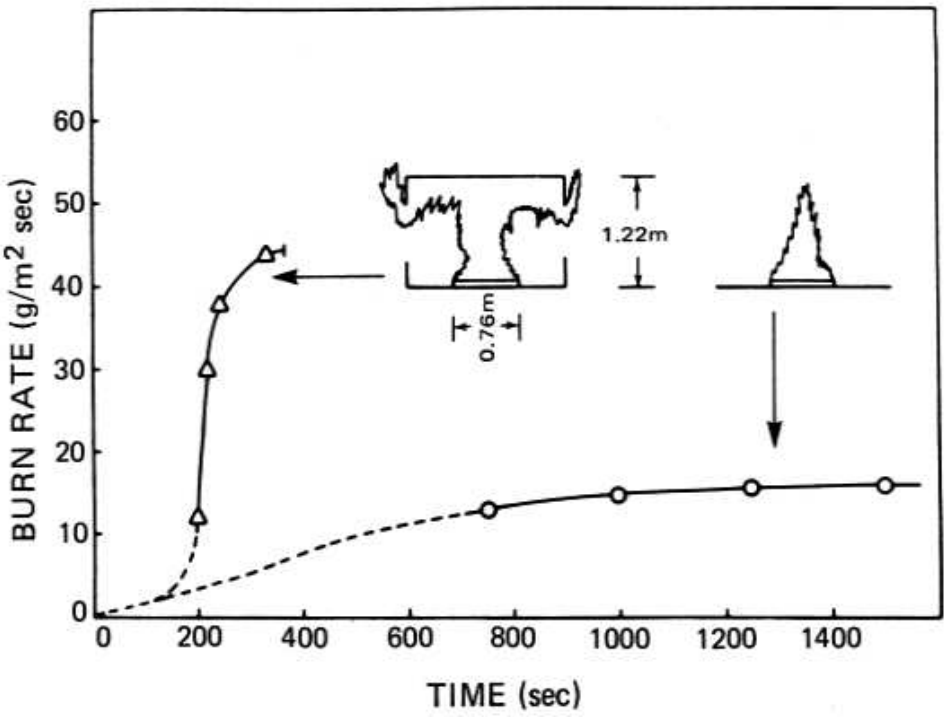

Figure 10

4.4 Flashover

Given the significant impact of "flashover" on the safety of building occupants, there has been a great deal of interest in comprehending the underlying process. The crucial question is whether a fire within a compartment will escalate to flashover or beyond. Trained firefighters can intervene to prevent flashover, but this can be a hazardous operation when dealing with large fires. In recent times, technology has been combined with an understanding of the mechanism, utilizing water sprays and mists to prevent flashover. This technique was originally developed in Sweden and demands a high degree of courage and skill.

Early research by Waterman emphasized that flashover will not occur unless the fire exceeds a certain critical size. Various indicators have been employed in experimental fires to define the beginning of flashover or the event itself. From small-scale compartment fires, Waterman concluded that a radiant heat flux of $20\ \frac{kW}{m^2}$ at floor level was a satisfactory criterion for the onset of flashover. This is substantially more than the minimum levels required for igniting most combustible solids, while somewhat less than the values associated with spontaneous ignition . However, a heat flux of this magnitude will significantly enhance the rate of flame spread. Other criteria based on experimental observations include an upper gas temperature of 600°C coinciding with flashover in compartments approximately 2.5 meters high, with flames typically emerging from the upper parts of ventilation openings. This is linked to the beginning of burning of the smoke layer beneath the ceiling and is followed by sustained external flaming as the fully developed fire begins, making it clear that flashover has occurred. For fire safety design

calculations, a radiant heat flux of 20 $\frac{kW}{m^2}$ provides a conservative criterion for the end of the growth period.
The modeling of this phase of the compartment fire is highly complex, as it must take into account the many and varied interactions. A simple zone model regards the flashover condition as a thermal instability, much like that which accounts for spontaneous ignition. Flashover is considered the stage in the fire when the rate of heat production within the compartment first surpasses the rate at which it can be lost. Under these conditions, the intensity and extent of the fire rapidly increase until the burning rate achieves a new state of quasi-equilibrium, typically limited by the rate of air supply (ventilation).
A significant amount of effort has gone into developing more sophisticated models to describe the pre-flashover fire. A major project at Harvard University, led by Emmons, resulted in the Harvard Fire Code, a "zone" model that has undergone successive modifications as our comprehension of the component parts of fire dynamics has improved. It has been further developed as "FIRST" at the National Bureau of Standards (now the National Institute for Science and Technology), and a modification was incorporated into HAZARD 1. The latest version of the Harvard zone model is the most advanced of its kind, incorporating, among other things, the fluid dynamics of gas flows in and out of the compartment, flame movement, radiation from the layer of hot, smoky gases beneath the ceiling, and combustible material's response to an increasing radiant heat flux. It is an invaluable tool for comprehending the mechanisms involved during the growth stage of a fire, but its value for design purposes remains to be proven. [13]

4.5 Mathematical Models

From an empirical standpoint, there is substantial evidence to suggest that a fire must reach a certain minimum size before the occurrence of flashover within a compartment. This aligns with Waterman's earlier findings, but it wasn't until 1981 that adequate data was collected to make some form of correlation. Upon examining a significant quantity of data regarding upper room-gas temperatures in enclosure fires that had not yet achieved flashover (where the upper temperature was less than 600°C), a simple zone model of the preflashover fire could be established. Based on the assumption that an upper gas temperature of 500°C would be a reliable indicator of the onset of flashover, the following equation was deduced:

$$\dot{Q}_{FO} = 610(h_k A_T A_w H^{1/2})^{1/2} \quad (1)$$

In this equation, $\dot{Q}_{FO}$ (in kW) represents the rate of heat release required to trigger flashover. A_T refers to the internal surface area, A_w and H denote the area and height of the ventilation opening, respectively, and h_k is an effective surface heat-transfer coefficient (in $\frac{W}{m^2K}$). For walls with a high thermal conductivity, h_k is proportional to (kρc)1/2. This suggests that compartments lined with materials of low thermal

inertia will probably experience flashover at lower $\dot{Q}_{FO}$ values. Other studies have also confirmed this, especially in measuring the time it takes for flashover to occur in compartments with varying thermal mass. This effect is associated with the exposed surface and not cavity insulation. Thus, the effect is expected to be negligible with the limited range of wall lining materials that are currently used, especially in the case of fast-growing fires.

The CIB (Conseil International du Bâtiment) conducted an international program of small-scale tests to examine the factors that influence the time it takes for flashover to occur. The results were subjected to statistical analysis, which revealed that the time to flashover is influenced by several factors, particularly those that cause rapid initial fire development and flame impingement on the ceiling. These include the size and location of the ignition source (or in terms of a real fire, those of the first ignited item), the height of the fuel bed, the fire properties of the wall lining materials, and the bulk density of the fuel, which affects the rate at which fire can spread from one item to another. This research, along with subsequent studies at the National Bureau of Standards (now NIST), has highlighted the importance of furniture spacing in the early growth of fire. If an item is more than 1 m away from an adjacent item, it is unlikely that the fire will spread directly from one item to another.

In the postflashover fire, all combustible surfaces are burning, and the average temperatures within the compartment will increase rapidly to a high level, which is determined by the rate of heat release within the compartment, the rate of heat loss, and the duration of burning. A flow of hot combustion products is established through the upper parts of the ventilation openings, above a neutral pressure plane. This flow is driven by the positive overpressures that are maintained in the upper part of the enclosure due to the buoyancy of the hot gases within the compartment. The corresponding pressure differential below the neutral plane causes air to be drawn into the fire, as seen in Fig 11. The high levels of radiative and convective heating within the compartment maintain a high rate of production of fuel volatiles ($\dot{Q}''_E$), and apply a thermal load on the compartment boundaries, which may eventually lead to their failure (as discussed below).

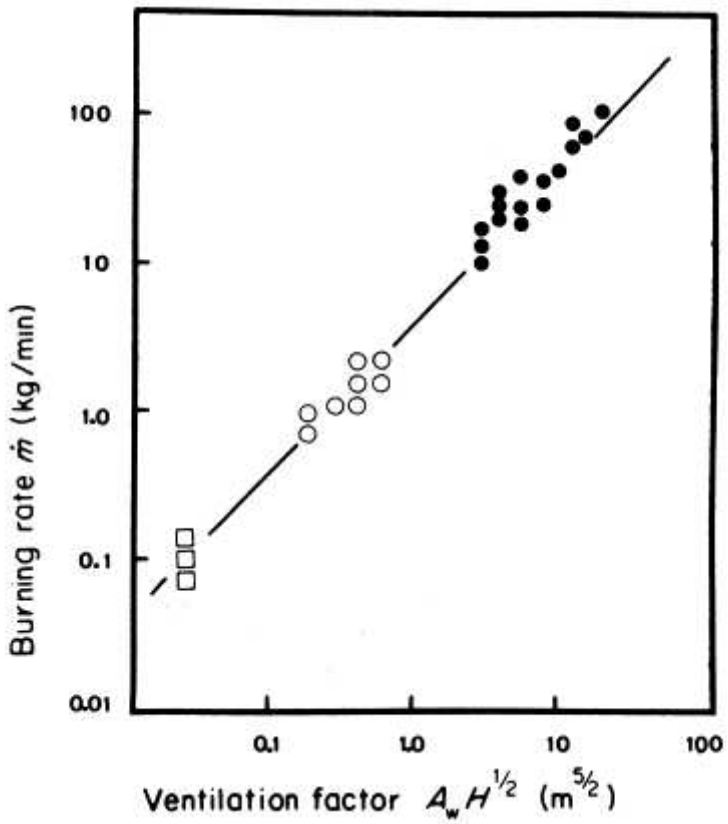

Figure 11

[13]

The amount of heat released in the room is not only determined by the rate of fuel vapor production, but also by the speed at which air is flowing into the room through the ventilation opening due to buoyancy-induced movements. Initial investigations of experimental fires that involved wooden cribs concluded that the rate of combustion could be linked to a ventilation factor $A_w H^{1/2}$, resulting in:

$$\dot{m} = 5.5 A_w H^{1/2} kg/min \quad (2)$$

A theoretical explanation for such a correlation can be found by analyzing the buoyancy-driven gas flows in and out of the room and assuming that stoichiometric combustion takes place, i.e., all of the oxygen entering the room reacts completely with an equal amount of fuel vapor. This implies that the rate of combustion and the rate of incoming air are directly linked, although there seems to be no logical reason for this to be the case. In reality, if the shape or nature of the fuel is altered, the correlation can drastically break down. For example, if the fuel was not in the form of wooden cribs but instead was present as wall-lining material, much higher

combustion rates could be attained, far exceeding the stoichiometric requirement for incoming air. As a result, some of the fuel vapours would not burn inside the room but instead would flow out of the ventilation opening and burn strongly as air is drawn into the plume, generating external flames.

The compartment's heat release rate depends not just on the rate of fuel volatiles production, but also on the speed at which air is drawn through the ventilation opening due to buoyancy-driven flows. Studies of wood crib fires suggest that the rate of burning is related to a ventilation factor, $A_w H^{1/2}$, as illustrated in Fig. 11. However, this relationship is only valid for the geometry and nature of the fuel used in the experiments. If the fuel is changed, the relationship may break down.

When unburnt fuel escapes through the ventilation opening, flames can form externally, but their size cannot be precisely calculated. Nevertheless, several contributory factors have been identified, including the quantity of unburnt fuel and the width of the opening. Correlations have been developed to estimate the fire protection necessary for external steelwork. If the vent area is made large enough, the rate of burning becomes independent of the ventilation factor, and the appearance is quite different from the fully developed ventilation-controlled fire.

Steady-state analyses of various scenarios have been carried out, which show the importance of the heat of gasification (L_v) in determining the nature of the fire. Fuels with low heat of gasification tend to have high rates of burning under steady-state conditions, as demonstrated by liquid fuels such as gasoline or hexane. The transition to the fully developed fire is prolonged by the natural delay that occurs before individual items reach their maximum rates of burning.

During the fully developed compartment fire, elements of structure are subjected to high thermal stress, and they must be designed to have a degree of fire resistance. Traditionally, fire resistance is measured in a large-scale standard test, which is an unsatisfactory approach as exposure within any of the existing test furnaces bears little resemblance to real fire exposure. It has been necessary to develop more severe fire resistance tests for petrochemical plants, where elements of structure may be exposed to hydrocarbon pool fires that produce very high temperatures much more rapidly than the typical compartment fire.

A design method for fire protection of structural steelwork in buildings was developed in Sweden in the 1970s. The potential fire exposure is first calculated from the rate of heat release, which depends on the total amount of fuel present, that is, the fire load. By carrying out numerical integration of the equations describing the rate of heat generation and the rate of heat loss from the compartment, the average gas temperature within the compartment can be calculated as a function of time from flashover.

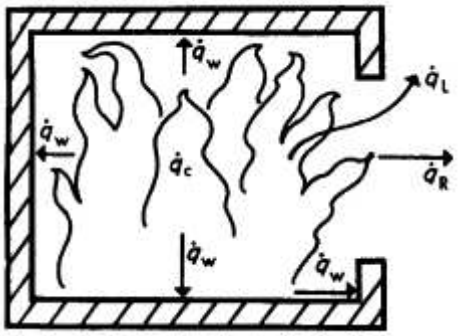

Figure 12

Figure 13 displays typical graphs for four different ventilation variables ($\frac{A_w H^{\frac{1}{2}}}{A_t}$, where A_t stands for the complete internal surface area) and a variety of fire load densities (measured in terms of available combustion energy, in $\frac{MJ}{m^2}$). Based on these graphs, one can determine whether a specific structural steelwork element will survive a particular fire using fundamental principles, as higher steel temperatures correspond to a reduced load-bearing capacity. In Sweden, this calculation approach is an acceptable substitute for conventional building codes, which incorporate fire-resistance tests but are rigid. However, both methods are fundamentally flawed since they only evaluate single structural elements (such as columns, beams, etc.) in isolation and overlook the interactions between structural components that occur in complex three-dimensional buildings, particularly during fires.

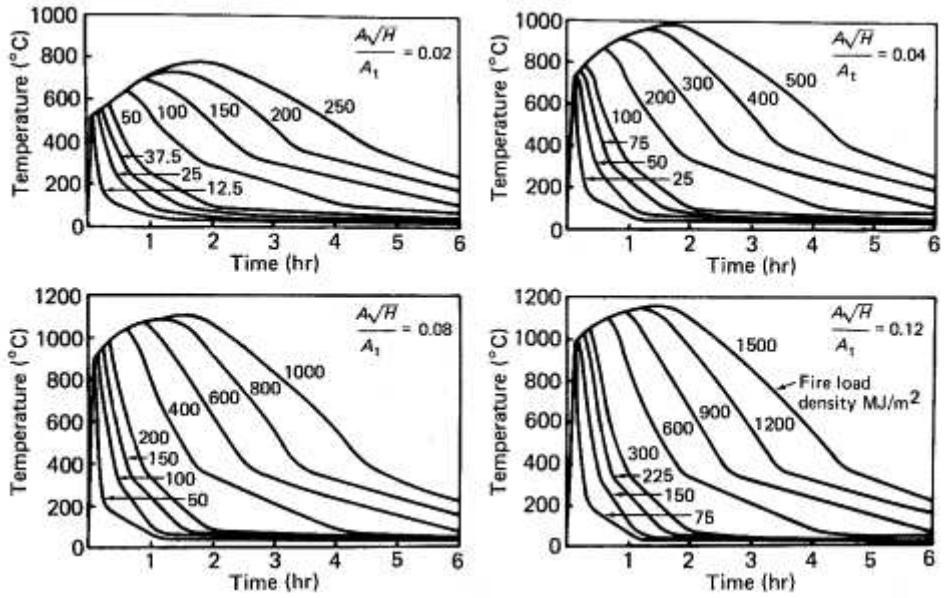

Figure 13

The term "fire severity" is commonly used, but it is rarely measured or quantified. It has been linked to the "fire resistance" needed to survive a fire. In Law's analysis of data from numerous experimental compartment fires, a correlation was found between t_F, the necessary fire resistance (measured in minutes), and the fire load (M_F) in terms of kilograms of wood equivalent, the ventilation area (A_w in m^2), and the total internal surface area of the compartment (A_T in m^2):

$$t_F = K' \frac{M_F}{(A_w A_T)^{1/2}} \quad (3)$$

where K' is a constant that is very close to 1. Other similar equations have been developed that aim to define a "time equivalent" based on a broader range of parameters, including the shape and thermal properties of the compartment's boundaries, but it is still uncertain how these can be used most effectively. Generally speaking, they do not apply to unprotected steel structures. [13]

4.6 Fire risk from EV batteries

Electric vehicles contain a significant amount of materials that can catch fire easily. These materials mainly include the power system (battery) and plastic components. The amount of polymer used in modern cars ranges from 100 to 200 kg, which is higher than the amount of gasoline used (less than 50 kg).

Regarding batteries, Lithium-ion batteries contain various materials that can catch fire easily. The heat generated from their combustion is influenced by several factors such as chemistry, packing, capacity, and state of charge (SOC). Generally, the heat generated from these types of batteries is about one order of magnitude lower than that of gasoline. For instance, a commercial pouch-type Lithium-ion battery with a capacity of 2.9 Ah (11 Wh) has a heat of combustion of about 4 MJ/kg, while it is about 2 MJ/kg for a 18650 cylindrical battery. The amount of thermal energy released from a battery fire, which includes both the internal heat and the flame heat sustained by the flammable gases, is much higher than the electrical energy stored in the battery. The amount of energy released from a battery fire can be 5-10 times higher than the stored electrical energy. [14]

5. Case Study

5.1 Description

By considering various potential significant incidents within galleries, several distinct scenarios are identified. The selected critical events include:

- Ignition of an electric vehicle in a gallery with ventilation system
- Ignition of an electric vehicle in a gallery without ventilation system

The first outcomes are analyzed based on two different jet fans positions within the gallery. In the first scenario, the ventilation system is placed near the vehicle, whereas in the second scenario, the fans are located far from that.

In order to simulate the vehicle, a parallelepiped (4 m x 1,8 m x 1,5 m) is built with the upper plane considered as the fire surface, as it is possible to see in the following figure.

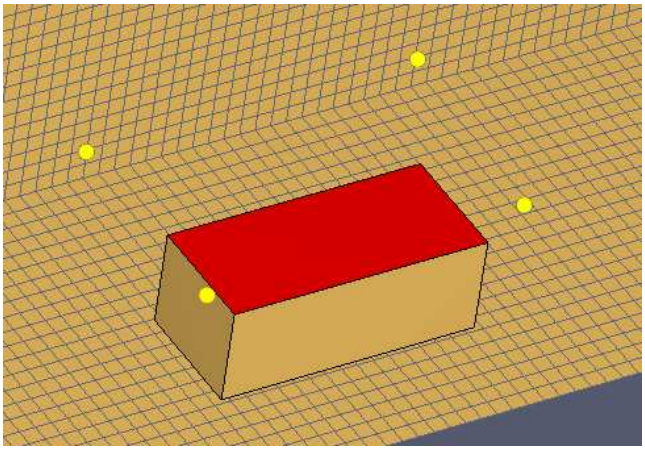

Figure 14

5.2 Approach and software

Fire engineering relies on appropriate models rooted in system physics, enabling dynamic and evolutionary fire predictions. This approach offers exceptional adaptability. By inputting various data (such as domain geometry calculations, ventilation conditions, fuel type and quantity, HRR curve over time), even highly intricate field models can be constructed.

A diverse range of models exists for predicting the dynamic evolution of fire, depending on the parameters and equations employed to solve the problem. At the parameter level, we can make an initial distinction between:

- Concentrated parameter models (or zones) that accurately solve one or more approximate equations containing operational parameters.
- Distributed parameter models (or field-solving models) that solve a set of exact equations.

Further classification can be made based on mathematical and physical principles, as well as complexity:

- Empirical and semi-empirical parametric models.
- Eulerian and Lagrangian numerical models.

Regarding simulations, two models are commonly used: "zone" and "field" models.

All Fire Dynamics Simulator (FDS) models involving combustion require the definition of a gas phase reaction, specifically the conversion of fuel into combustion products. In this study, we explore a simplified chemical approach. The fuel components include carbon, hydrogen, oxygen, and nitrogen, which react with oxygen to produce water, carbon dioxide, carbon monoxide, and nitrogen. Two additional parameters need to be specified: the heat of combustion and the radiative fraction. The SFPE Handbook of Fire Protection Engineering offers guidance on determining the heat of combustion.

PyroSim serves as an FDS precompiler, designed specifically for processing input data for FDS. Its graphical interface during the pre-processing phase greatly facilitates data assessment and decision-making. Modifying data in real-time and checking the resulting changes to the structure's geometry elements (such as mesh adjustments or outline conditions) is relatively straightforward. Therefore, PyroSim is an ideal tool for fitting the results of this thesis. Moreover, by employing the same equations as FDS for data processing and utilizing the same post-processor (Smokeview), PyroSim is particularly suitable for simulating medium to slow fire evolution and studying smoke propagation.

PyroSim offers four editors for the developed fire model: the 3D View, 2D View, Navigation View, and Record View. If an object is added, removed, or selected in one view, the other views will simultaneously reflect the change.

5.3 Software setup

In Pyrosim, you can generate a mesh to establish a specific control region where the simulations will take place. In this case the mesh has a length of 200 m, selected to prevent overly long simulations while still achieving accurate outcomes. In this specific instance, the mesh is divided into three sections, as illustrated in Figure 14.

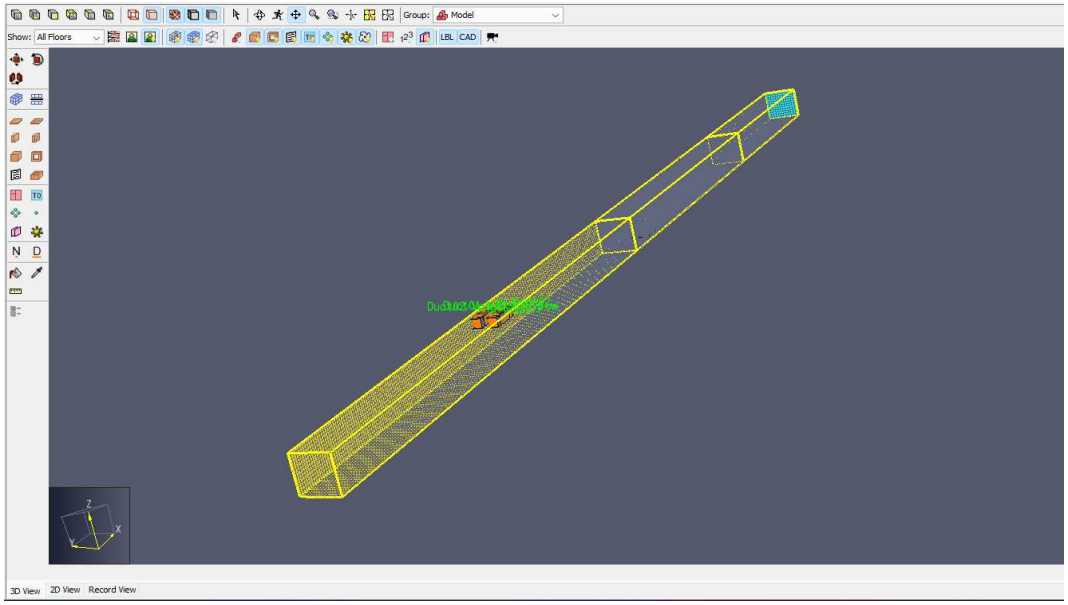

Figure 15

The mesh consists of 178560 cells. One section is more substantial, housing 138240 cells with a cell size of 0.25 x 0.25 x 0.25 m, while the other two sections are less dense with a cell size of 0.5 x 0.5 x 0.5. The fire and other critical components will be located within the thicker section. The disparity in mesh density can be observed in Figure 15.

To determine this mesh configuration, a trial and error approach was employed. This allowed for minimizing simulation complexity while still obtaining satisfactory results. Various simulations will be conducted with different positions for the burned car, necessitating the adjustment of the meshes accordingly. Once the correct geometry was established, all other elements were placed in their respective positions.

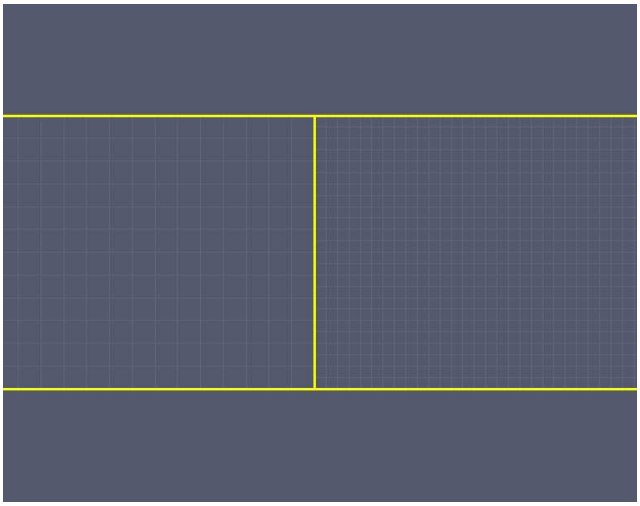

Figure 16

5.4 Tunnel

The underground passage is constructed with the following primary characteristics:

- One lane with a width of 4,6 meters.
- As per regulations, the minimum required height is 4.5 meters. However, in this case, the height has been established at 6 meters.
- To achieve precise outcomes without excessively long simulations, a gallery measuring 200 meters in length has been erected.
- In order to ensure the tunnel's safety, an emergency exit has been installed [15]

Concrete has been chosen as the material for constructing the gallery's structure.

5.5 Ventilation

The recent EU directive (EU 2004/54/CE) regarding the minimum safety standards for tunnels within the trans-European road network recognizes the importance of ventilation and ventilation control. This directive addresses the need for systems that can manage the emission of pollutants from vehicles during regular and congested operation, as well as the control of heat and smoke in the event of a fire [16].

Tunnel ventilation is based on the application of one of two principles:
dilution of polluted air/smoke and removal of polluted air/smoke.

During normal operations, dilution is typically employed to maintain visibility and air quality above the specified threshold. In emergency situations, air renewal techniques such as smoke and air extraction are used to handle smoke. Dilution can also improve habitability by reducing harmful gas concentrations. Consequently, contaminated air is replaced with cleaner or smoke-free air, which is either mechanically supplied or brought in through the tunnel portals [16].

Since the considered gallery is unidirectional, longitudinal ventilation using jet fans has been adopted. This system ensures a flow along the tunnel's axis. Two jet fans, consisting of an impeller driven by an electric motor, are positioned within the tunnel. The rotating blades of the fans generate airflow. Unlike traditional fans, these jet fans are not enclosed within ducts.

To provide ventilation for the unidirectional gallery, a longitudinal flow system with jet fans has been implemented. This system ensures that the air flows longitudinally along the axis of the tunnel. Two jet fans have been installed, each consisting of an impeller driven by an electric motor with blades that generate airflow when they rotate. These fans are not ducted like traditional fans.

To select the appropriate type of fan for the gallery, the following factors need to be considered:

- Type of fan selected, along with specified flow rate, pressure, number of revolutions, supply voltage, and frequency.
- Orientation of the fan.
- Construction of the fan.
- Position of the engine.
- Accessories needed for the fan.

The FDS model requires the flow rate of the fan as an input parameter. This flow rate can be calculated using the following formula:

$$Q_V = V * R \qquad (4)$$

Where Q_V represents the volumetric flow rate of the fan (in cubic meters per second), V represents the volume of the environment (in cubic meters), and R represents the number of air changes per hour.

The setup includes a pair of jet fans, that activate three minutes after initiation, with a ramp-up time of 30 seconds. The volumetric flow rate is 24 $\frac{m^3}{s}$, and the jet fans are installed on the upper part of the gallery.

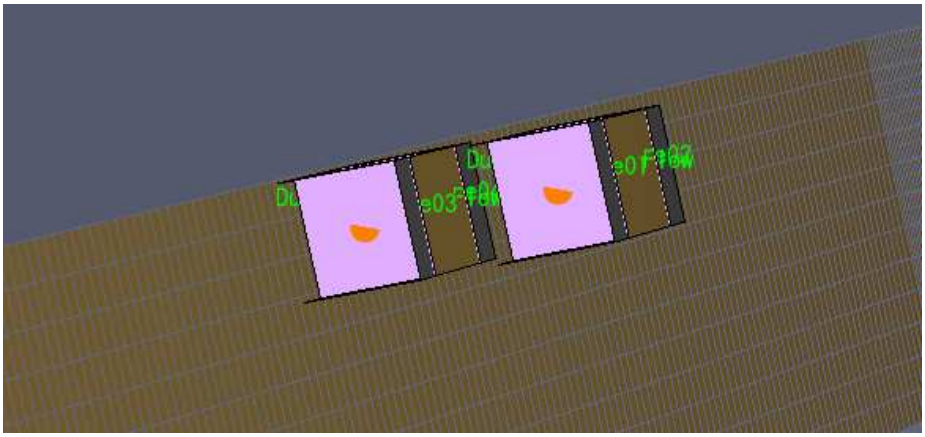

Figure 17

Due to the influence of buoyancy forces, smoke generated by a fire in the tunnel tends to rise. If the airflow is stagnant or moving very slowly, the smoke will spread along the ceiling on both sides of the fire. In the case of sloping tunnels, buoyancy effects can cause the bulk flow in the tunnel to migrate upwards, following the tunnel gradient, resulting in the smoke being carried in the same direction. Behind these layers of smoke or towards the fire, fresh air is drawn in. This stratification creates a division between the warmer lower layers and the hotter upper layers.

As demonstrated in the simulations, when the affected section of the tunnel is ventilated, a longitudinal airflow propels the smoke downstream through the tunnel while slowing its movement on the upstream side.

5.6 Materials

In 2020, NMC batteries accounted for 72% of the batteries used in electric vehicles (EVs), making them the most commonly used type in the automotive industry. NMC batteries have a cathode composed of nickel, manganese, cobalt, and lithium, which allows them to achieve a very high specific energy of up to 220-240 Wh/kg. This characteristic provides a significant competitive advantage for cars, as it allows for the installation of more energy in the vehicle compared to other lithium-based technologies. Despite this, NMC batteries have a relatively small weight and volume, enabling the storage of large amounts of energy. Various compositions of NMC cathodes exist, including NMC 111 (with 33.3% nickel, manganese, and cobalt each), NMC 622 (with 60% nickel, 20% manganese, and 20% cobalt), and NMC 811 (with 80% nickel, 10% manganese, and 10% cobalt). Among these, NMC 622 cells are the most commonly used. A typical battery with a capacity of 60 kWh contains approximately 185 kg of minerals in each cell, excluding the electrolyte, binder, separator, and battery pack casing. The detailed percentages can be found in Table 1.

Mineral	Cell Part	Amount Contained in the Avg. 2020 Battery (kg)	% of Total
Graphite	Anode	52kg	28.1%
Aluminum	Cathode, Casing, Current collectors	35kg	18.9%
Nickel	Cathode	29kg	15.7%
Copper	Current collectors	20kg	10.8%
Steel	Casing	20kg	10.8%
Manganese	Cathode	10kg	5.4%
Cobalt	Cathode	8kg	4.3%
Lithium	Cathode	6kg	3.2%
Iron	Cathode	5kg	2.7%
Total	**N/A**	**185kg**	**100%**

Table 1

The cathode, considered the primary and costly component of the battery, exhibits the highest range of mineral variations. The battery's specific composition, as considered in the model, can be found in Table 2.

	Mass Fraction	Material
1	0,282	Graphite
2	0,157	NICKEL
3	0,108	Copper
4	0,054	Manganese
5	0,043	Cobalt
6	0,032	Lithium
7	0,027	Iron
8	0,189	Aluminum
9	0,108	STEEL
*		

Table 2

The model incorporates all of this information. The proportion of battery weight in an electric vehicle (EV) can vary depending on the specific make and model. In this case a lithium-ion battery pack in the car weights approximately 272 kg, which accounts for roughly 20% of the vehicle's total weight (1352 kg). The remaining materials utilized in the car are outlined below:

- Steel: comprising approximately 55% of the vehicle's body and frame, steel is employed to enhance strength and durability.
- Aluminum: constituting nearly 10% of the vehicle, aluminum is utilized in certain components like wheels and suspensions to reduce weight and enhance fuel efficiency.
- Plastics: accounting for 8% of the car, plastics are used for interior trim and exterior panels due to their lightweight nature and durability.
- Glass: making up approximately 4% of the vehicle, glass is used for windows and the windshield.
- Rubber: comprising roughly 2% of the vehicle.
- Others: accounting for 1% of the vehicle's components.

Table 3 provides an overview of all these components as integrated into the model, summarizing the considerations discussed in this section.

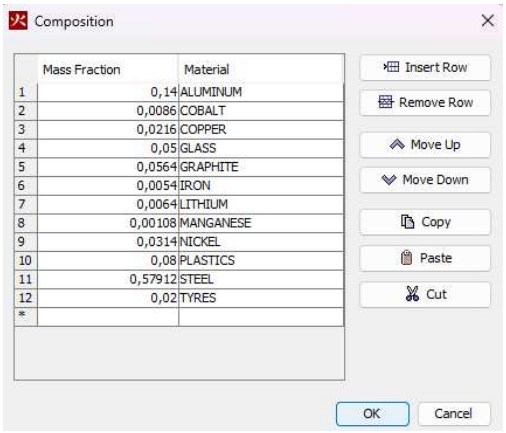

Table 3

On what concerns the Heat Release Rate (HRR), when it comes to electric vehicles, the heat release rate per unit area (HRRPUA) can exhibit significant variations depending on the battery chemistry and the state of charge. As a rough estimate, the HRRPUA in a fully developed fire is generally around 100 $\frac{kW}{m^2}$ [17]. However, it's worth noting that electric vehicle fires tend to have a comparatively slower ramp-up time in comparison to fires involving gasoline or diesel vehicles. This can be attributed to the design of battery systems, which typically incorporate safety measures to prevent thermal runaway and overheating. Therefore, a ramp-up time of 150 seconds is taken into consideration.

5.7 Devices

In order to gain a better understanding of the fire's progression within the tunnel, simulations incorporate additional devices and controls.

Devices refer to instruments that enable the precise measurement of selected parameters. One such device is the thermocouple, which serves as a temperature sensor in various settings. Comprising two dissimilar metal wires joined at one end, thermocouples are connected to a measuring device on the other end. When exposed to a temperature difference, an electromotive force (EMF) is generated at the junction of the wires, proportional to the temperature disparity. Thermocouples are popular due to their affordability, durability, wide temperature range, and rapid response time. They can measure temperatures ranging from as low as -200°C to as high as 2500°C, depending on the thermocouple wire materials used. However, factors such as aging, contamination, and electromagnetic interference can affect their accuracy, necessitating consideration during calibration and usage of the sensors [18].

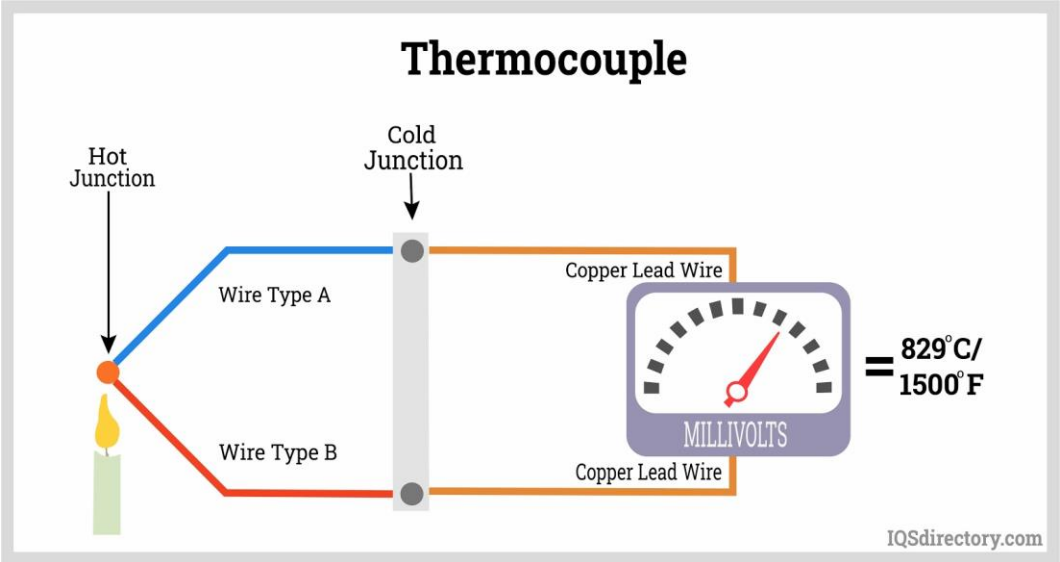

Figure 18

Strategically positioned thermocouples are utilized to monitor the temperature evolution within the tunnel over time. In this case, eight thermocouples are employed: four near the car, close to the fire, one near jet fans, one near the emergency exits, one at the inlet of the tunnel and one at its outlet. The positions of these thermocouples can be observed in Figure 19, 20 and 21.

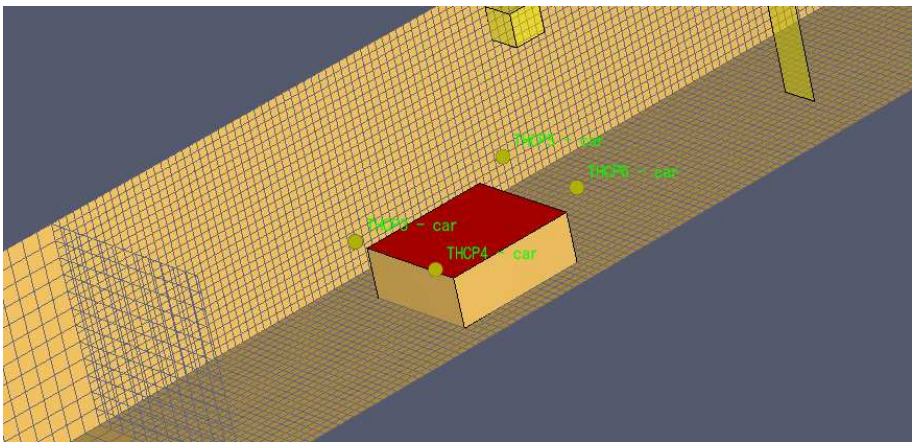

Figure 19

Figure 20

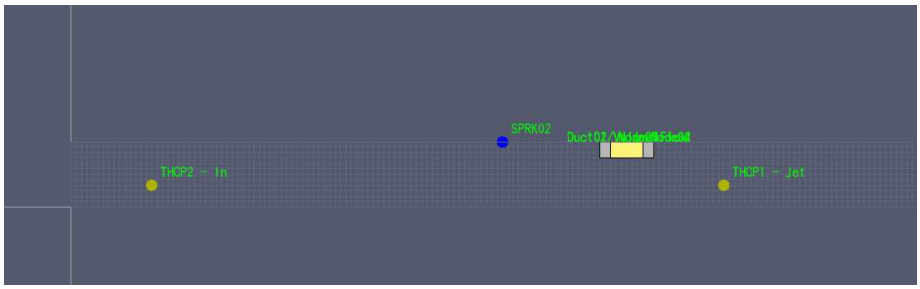

Figure 21

Another important device employed is the calorimeter, which measures the amount of heat released or absorbed during a chemical or physical process. The calorimeter operates by measuring the temperature change that occurs when a reaction takes place or a substance is heated or cooled. The most common type of calorimeter is the constant pressure calorimeter, also known as a bomb calorimeter. This device typically consists of a sealed container, often made of stainless steel, filled with a sample of the substance to be analyzed and a known quantity of oxygen. The bomb is placed in a water bath, and the temperature of the water is measured before and after the reaction occurs.

When the sample ignites, reacting with oxygen, heat is produced, raising the water temperature [19]. By measuring the temperature change and knowing the calorimeter's heat capacity, the heat released by the reaction can be calculated using the formula:

$$\Delta H = -mC\Delta T \quad (5)$$

where ΔH represents the heat released (in Joules), m is the mass of water in the calorimeter (in kilograms), C is the specific heat capacity of water ($4{,}18 \cdot 10^3$ J/kgK), and ΔT is the rise in temperature of the water in the calorimeter (in Kelvin).

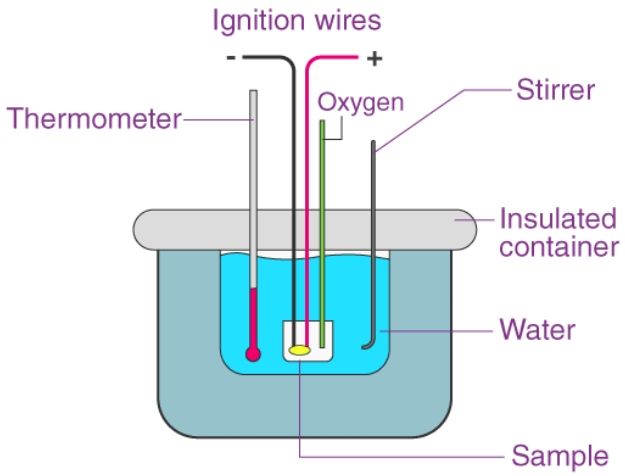

Figure 22

In this model the device is positioned near the fire, as it is shown in Figure 22.

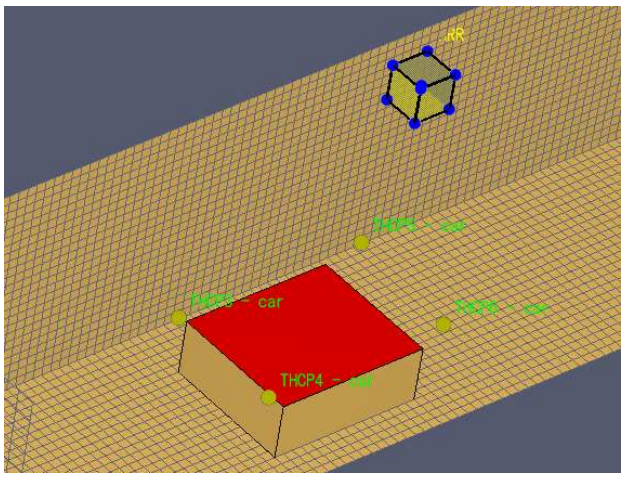

Figure 23

A flow measuring device is also utilized to determine the rate at which a fluid, such as a gas or liquid, is flowing through a pipe or channel. Thermal flow meters are considered in this case, which use the principle of thermal dispersion to measure fluid flow rate. These devices incorporate two temperature sensors: one heated and one unheated. As the fluid flows over the heated sensor, heat is conducted away from the sensor, resulting in a temperature difference between the two sensors. The heat loss from the sensor is proportional to the fluid's flow rate [20]. By measuring the temperature difference and the power required to maintain the sensor at a constant temperature, the flow rate of the fluid can be calculated. In this case it is located near the fire.

Furthermore, fire protection apparatus known as sprinklers are integrated into the model. Sprinklers function by spraying water or other extinguishing substances to contain or extinguish a fire. Typically, sprinkler systems consist of a network of pipes connected to a water source and controlled by a valve. When a fire is detected, the sprinkler heads on the pipes discharge water [21]. Sprinklers are designed to activate at specific temperatures, typically ranging from 68°C to 165°C. The heat from the flames triggers the sprinkler heads, initiating the release of water, which cools the fire, prevents its spread, and reduces property damage while lowering the risk of injury or fatalities.

Figure 24

Two sprinklers with specific characteristics are added to the model, as shown in the following figures.

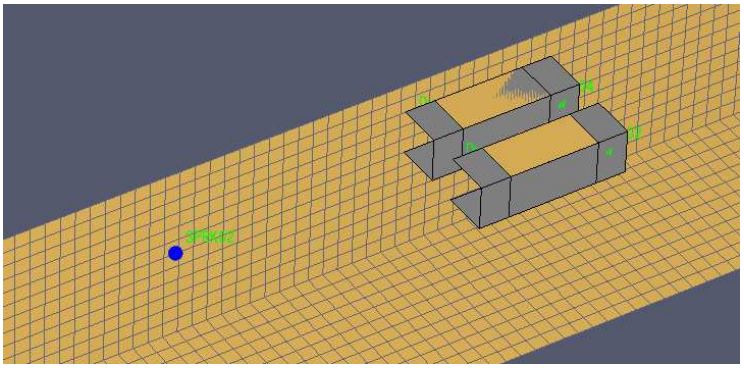

Figure 25

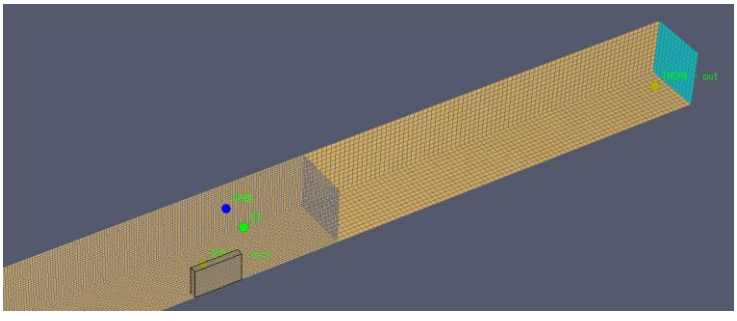

Figure 26

Another important device incorporated is the smoke detector, which detects smoke and provides a warning when a fire is present. Smoke detectors are typically installed high on walls or on ceilings in residential and commercial buildings, including road galleries. Most smoke detectors function by ionizing the air using a small radioactive source, such as americium-241. When smoke particles enter the detector, they interrupt the ionization process, triggering an alarm. Other types of smoke detectors employ optical or heat sensors. Smoke detectors play a crucial role in fire safety, potentially saving lives and protecting property from harm [22]. In the model, a smoke detector is positioned near jet fans attached to the tunnel's ceiling. The selected type is the clear ionization I1, chosen for its faster response compared to other types.

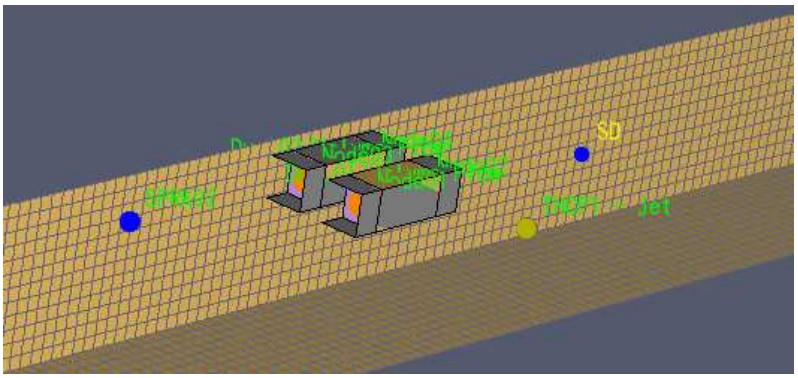

Figure 27

6. Results

Three different cases are analyzed with the simulation time of 60 seconds. A higher time could better study the models but the GPU and time requirements were very problematic. Therefore this analysis is focused on the very first time after the ignition.

6.1 Case A: no ventilation system

The first simulation is performed with no ventilation system, in order to underline the importance of these components.

Figure 28

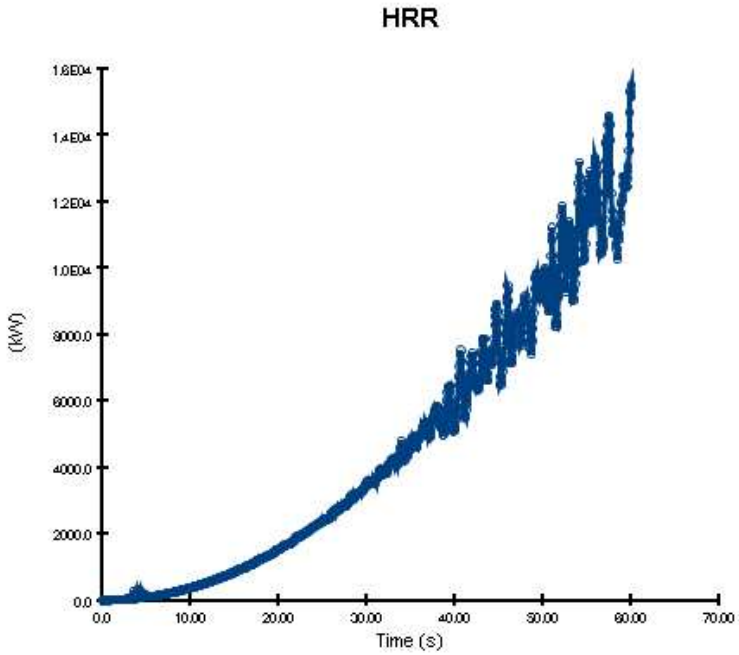

Figure 29

It is possible to analyse the value of HRR that is very high, over expectation.
This is also confirmed in the temperature's values reported by the thermocouples near the car.

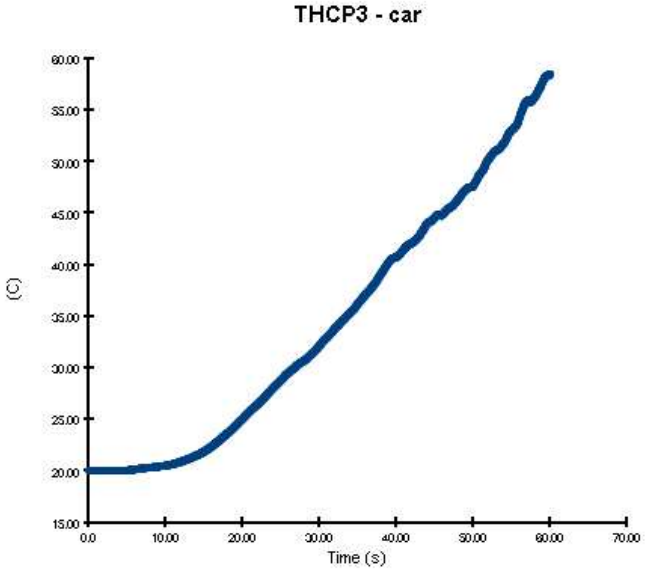

Figure 30

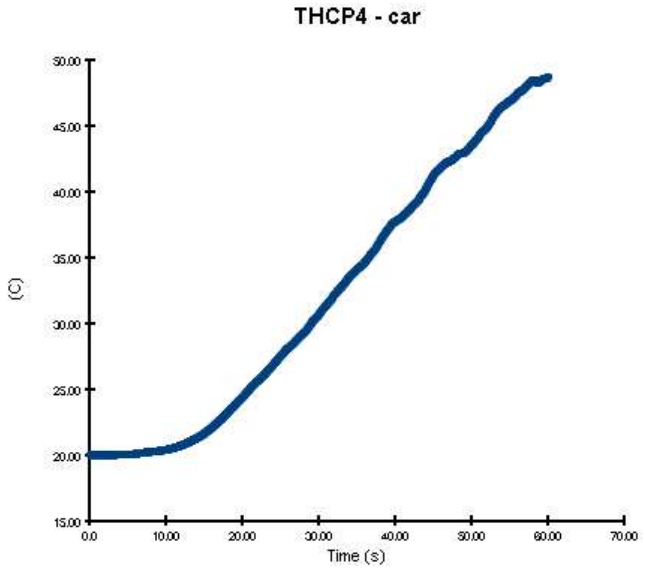

Figure 31

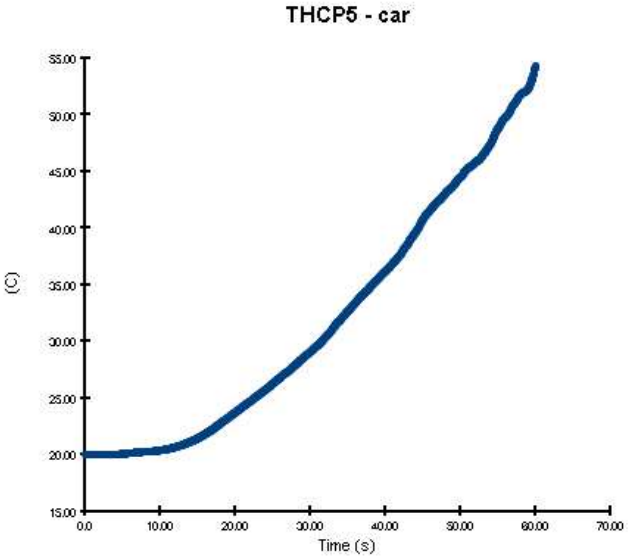

Figure 32

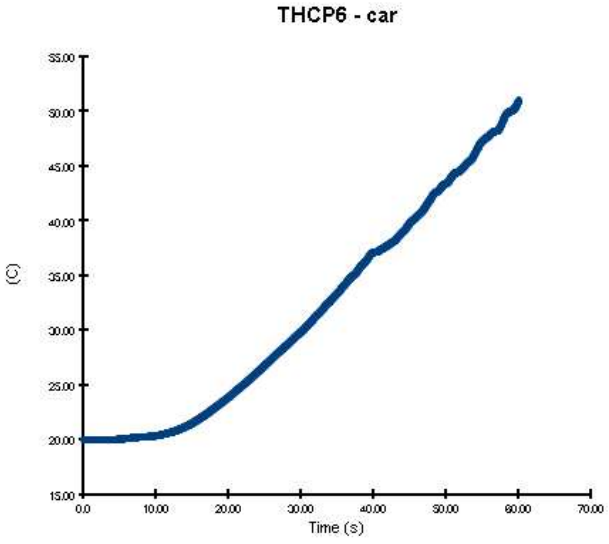

Figure 33

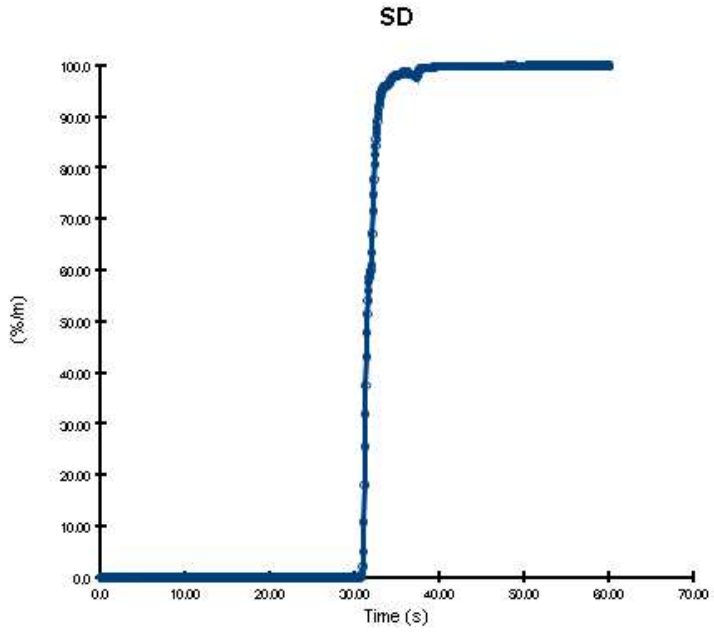

Figure 34

Another focus can be done on what concerns the smoke detector. It is located in the tunnel with a distance of about 20 m from the vehicle and, as it is shown in Figure 34, it is activated after 30 s from the ignition.

6.2 Case B: ventilation system far from the fire

The second case is performed with the implementation of a couple of jet fans as a ventilation system. They are located in the first part of the tunnel, with a distance of about 50 m from the fire.

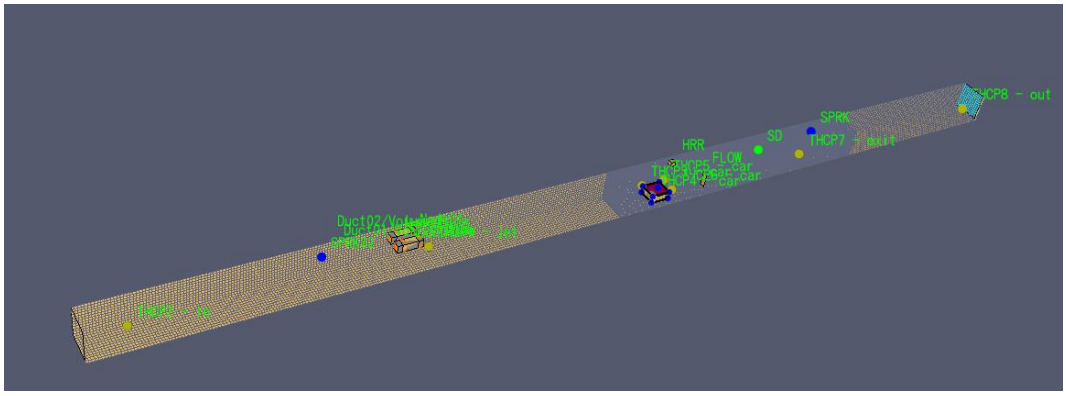

Figure 35

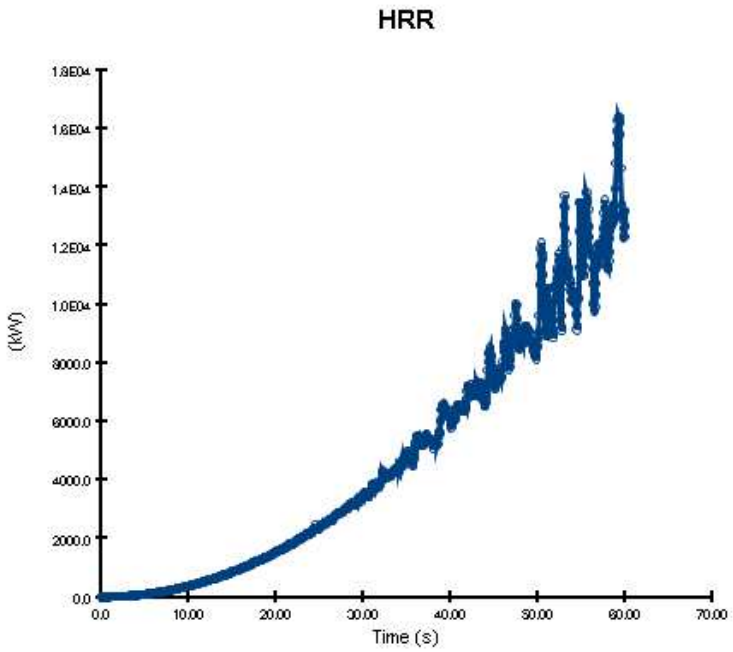

Figure 36

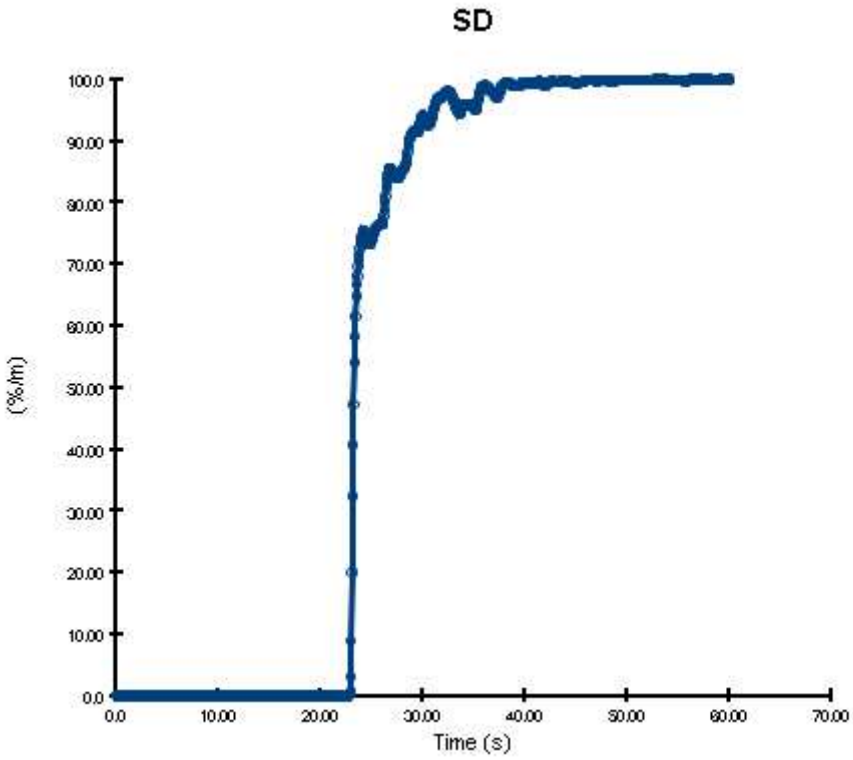

Figure 37

Analyzing the smoke detector system in Figure 37 it is possible to notice that the jet fans produce an advance of about 7 seconds in the smoke detection.

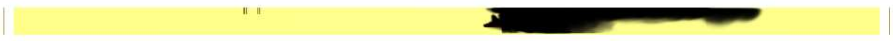

Figure 38

6.3 Case C: ventilation system near the fire

In this simulation the couple of jet fans is located near the electric vehicle, therefore near the fire, as represented in Figure 39.

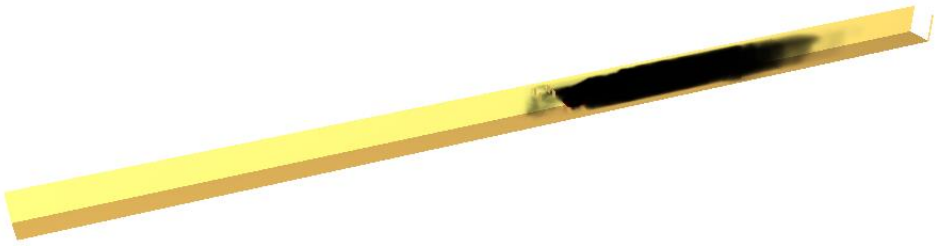

Figure 39

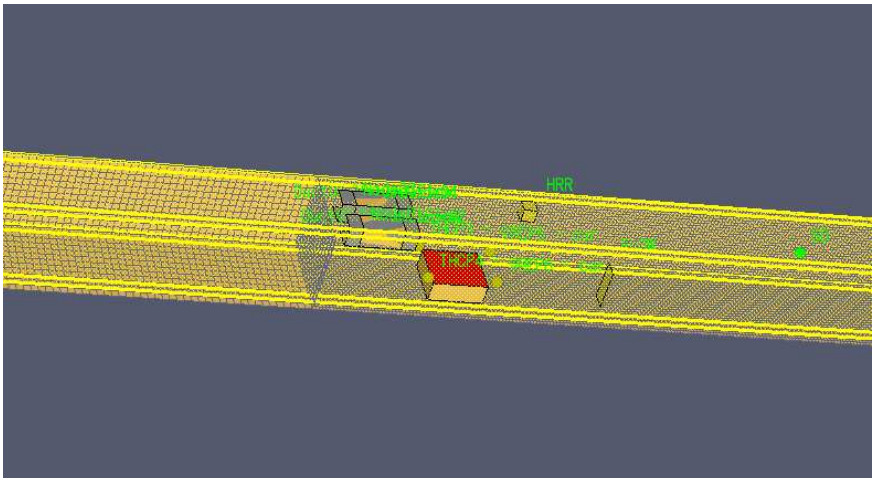

Figure 40

It is possible to see the diagram of the HRR in figure 41.

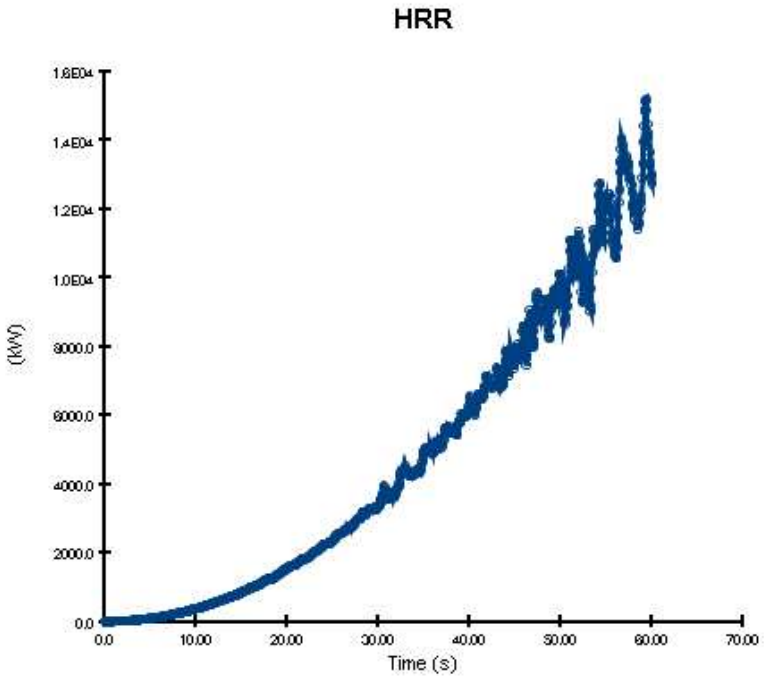

Figure 41

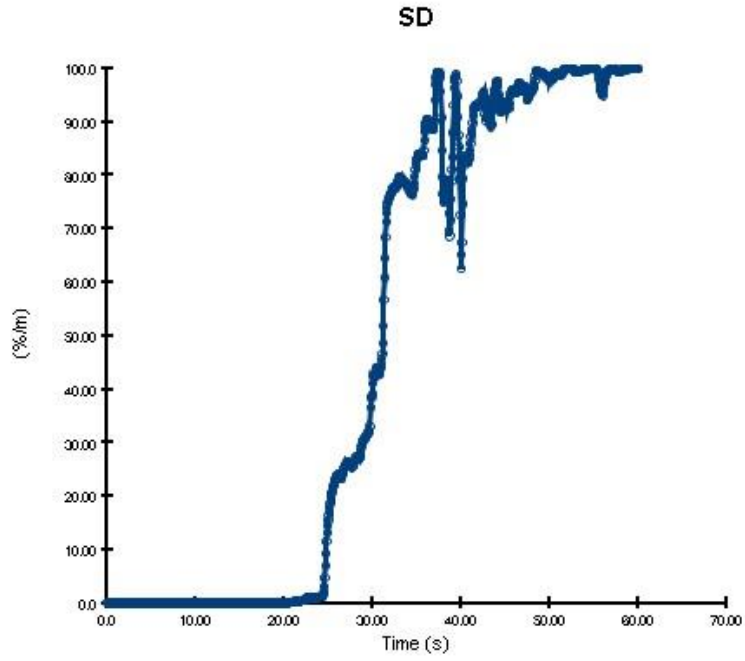

Figure 42

7. Conclusions

EV-related incidents remain a topic of great interest, leading individuals to exercise increased caution in their response. While it is undeniable that electric vehicles (EVs) pose additional risks, there is insufficient evidence to support the notion that EVs are less safe than their traditional counterparts. Nonetheless, as the population of EVs expands, instances of failures are likely to become more frequent.

Simulation software such as Pyrosim can help because of the huge quantity of data that can be got. The optimal approach entails confronting this issue head-on by implementing safety measures and protocols that minimize hazards to manageable levels. It is important to continue the study of the fire risks caused by electric vehicle and it is only through such efforts that society can attain a comparable level of confidence in EVs as it does in conventional vehicles.

8. Bibliography

[1] A.Lecocq, G.G.Eshetu, S.Grugeon, N.Martin, S.Laurelle, G.Marlair *"Scenario-based prediction of Li-ion batteries fire-induced toxicity"*

[2] Hansen, J., *et al.* (2010). Global surface temperature change. *Reviews of Geophysics,* 48.

[3] NASA Earth Observatory (2015, January 21) Why So Many Global Temperature Records?

[4] NASA Earth Observatory (2010, June 3) Global Warming.

[5] NASA Earth Observatory (2023, January 13) 2022 Tied for Fifth Warmest Year on Record.

[6] NASA Goddard Institute for Space Studies (2023) GISS Surface Temperature Analysis (GISTEMP).

[7] NOAA National Centers for Environmental Information (2022, January 10) Assessing the Global Climate in 2021.

[8] Alan Jenn, The Conversation

[9] Jeremy Laukkonen, "EV (BEV) vs PHEV vs FCEV vs Hybrid: What's the Difference?"

[10] Iclodean C., Varga B., Burnete N., Cimerdean D., Jurchis B. "Comparison of different battery types for Electric Vehicles"

[11] Linden, David and Reddy Thomas B. (2002). Handbook of Batteries 3rd Edition. McGraw-Hill, New York, chapter 35.

[12] Clean Energy Institute, "What is a lithium-ion battery and how does it work?"

[13] D.D. Drysdale, "Fire Dynamics", in Encyclopedia of Physical Science and Technology (Third Edition), 2003

[14] Peiyi Sun, Roeland B., Huichang N., Xinyan H. "A review of battery fires in electric vehicles" (2020)

[15] "Manuale delle gallerie stradali: uscite d'emergenza.". Available at https://tunnels.piarc.org/it/operativita-e-requisiti-di-sicurezza-sistemistrutturali/uscitedemergenza#:~:text=La%20distanza%20ottimale%20tra%20due,dall'accesso%20ai%20locali%20tecnici.

[16] PIARC Technical Commitee 3.3 Road Tunnel Operation.
"Road tunnels: operational strategies for emergency ventilation."

[17] National fire protection association. "Guide for Fire and Explosion Investigations". Available at: https://www.nfpa.org/codes-andstandards/all-codes-and-standards/list-of-codes-andstandards/detail?code=921

[18] "Thermocouple" .
Available at: https://en.wikipedia.org/wiki/Thermocouple

[19] "Calorimeter"
Available at: https://en.wikipedia.org/wiki/Calorimeter

[20] "Thermal mass flow meter"
Available at: https://en.wikipedia.org/wiki/Thermal_mass_flow_meter

[21] "Sprinkler". Available at: https://it.wikipedia.org/wiki/Sprinkler

[22] "Smoke detector".
Available at: https://en.wikipedia.org/wiki/Smoke_detector

[23] National Fire Protection Association (NFPA) (2019): Guide for Fire and Explosion Investigations. Quincy, MA: Author. National Transportation Safety Board (NTSB) report